GERMAN - MONGOLIAN INSTITUTE
FOR RESOURCES AND TECHNOLOGY

Design and analysis of hybrid vehicle transmission

by

TEMUULEN Khorloorentsen

B2200531

A Bachelor Thesis

The present work was submitted to the Faculty of Mechanical Engineering

BACHELOR IN MECHANICAL ENGINEERING

of the German Mongolian Institute for Resources and Technology

Supervisor 1 / Examiner 1: Phd Kim Young Suk

Supervisor 2 / Examiner 2: Prof. Phd Sungchil Lee

Ulaanbaatar / Nalaikh

2026

Statutory Declaration

Khorloorentsen ,Temuulen	B2200531
Last Name, First Name	Student ID Number

I hereby affirm in lieu of an oath that I provided the submitted bachelor thesis

Design and analysis of hybrid vehicle transmission

I did not use any sources other than those stated. Where AI tools were used, they were used solely for the purposes of language support and editorial assistance. All AI-assisted content was carefully reviewed, verified, and revised under my own judgment and responsibility. The intellectual contribution, core arguments, analysis, and conclusions of this thesis remain entirely my own. The work was not submitted in the same or similar form to any examination authority.

Ulaanbaatar,Mongolia, .04.2026	
Place, Date	Signature

Acknowledgement

This thesis would not have been possible without the support and help of many people around me, and I would like to take this opportunity to thank them all.

First, I am very thankful to my two supervisors for their guidance, patience, and valuable feedback throughout this research. Their advice and time helped me stay on the right track and improve my work at every step.

I would also like to thank my teachers and faculty members for sharing their knowledge and for always being supportive during my studies.

My deepest thanks go to my parents for their love, care, and support throughout my life. They always encouraged me to keep going, even during the most difficult times, and this work is dedicated to them.

I am also grateful to my siblings and family for being there for me and for their patience and support while I was busy with this thesis.

To my friends, thank you for your encouragement, your company, and for always cheering me up when things got tough.

Lastly, I would like to acknowledge the use of various internet resources and online academic databases that were helpful in gathering information and supporting the research process. All sources were carefully reviewed and properly referenced throughout this thesis.

Abstract

The global automotive industry faces mounting pressure from emissions regulations, rising fuel costs, and environmental awareness. Hybrid electric vehicles (HEVs) represent the most commercially mature transition technology, and at the core of every full hybrid powertrain is a transmission system capable of managing power from two energy sources continuously and efficiently.

This thesis presents the complete design and engineering analysis of a hybrid vehicle transmission, with specific focus on the Electrically Controlled Continuously Variable Transmission (e-CVT). The work begins with a comprehensive review and comparison of all five major automotive transmission types — manual, automatic, dual-clutch, conventional CVT, and e-CVT — establishing the e-CVT as the uniquely suitable architecture for hybrid applications.

The e-CVT mechanism is then analysed in full depth, including the Willis equation governing planetary gear kinematics, all five operating modes, and power flow analysis. A three-stage systematic design methodology is applied: Stage 1 selects the optimal gear ratio k=2.600 from a comprehensive scoring of all 95 valid designs in the automotive range; Stage 2 confirms the tooth counts Ns=20, Np=16, Nr=52 satisfying all geometric and assembly rules; Stage 3 calculates complete AGMA dimensions and verifies structural integrity using formulas from Myszka, Machines and Mechanisms (4th Ed.), Table 10.3.

All gear force and stress calculations are derived from first principles. At m=3 mm the Lewis bending stress is 57.5 MPa (sun) and 62.6 MPa (planet) against a limit of 207 MPa, the Hertz contact stress is 389.9 MPa against a limit of 733 MPa, and the contact ratio is 1.528 confirming robust meshing. The extended chapters cover involute tooth mathematics, material selection, manufacturing, kinematics superposition, safety factors, and production vehicle comparison.

Table of Contents

List of Figures i

List of Tables ii

Nomenclature iii

Abbreviations v

1. Introduction 1

    1.1 Background and Motivation 1

    1.2 The e-CVT Principle 2

    1.3 Thesis Objectives 2

    1.4 Thesis Scope and Limitations 3

2. Types of Automotive Transmissions 4

    2.1 Manual Transmission 4

    2.2 Automatic Transmission 4

    2.3 Dual-Clutch Transmission 4

    2.4 Conventional CVT 5

    2.5 Comparison of Transmission Types 5

3. The e-CVT — Mechanism and Operation 6

    3.1 Overview and History 6

    3.2 Planetary Gear Set Fundamentals 7

    3.3 Willis Equation and Power Flow 8

    3.4 Operating Modes 8

    3.5 Efficiency Characteristics 9

    3.6 How the e-CVT Works — Step-by-Step Power Flow 10

    3.7 Industry e-CVT Architectures: Power-Split Modes and the Mechanical Point 11

4. Literature Review 15

    4.1 Hybrid Vehicle Powertrain Development 15

    4.2 e-CVT Gear Set Design 15

    4.3 Gear Design Standards and Methodology 16

    4.4 Gap Identified 16

4.5 Finite Element Analysis in Gear Design 16
4.6 Module Selection and Gear Geometry Optimisation 17
4.7 Planetary Gear Stress in Hybrid Powertrain Applications 18
4.8 Review Summary and Positioning of This Work 18
5. Gear Ratio Selection — Stage 1 19
5.1 What the Gear Ratio k Controls 19
5.2 Scoring Methodology — Five Weighted Criteria 19
5.3 Design Search – All Valid Gear Ratios 20
5.4 Scatter plot – All Valid Designs Coloured By Score 20
5.5 Bar Chart — Top 20 Designs 21
5.6 Per-Criterion Comparison — Why Ns=20/Np=16/Nr=52 is Selected 22
5.7 Why Ns=20/Np=16/Nr=52 is the Final Selection 23
5.8 Top 10 Ranked Designs — Full Data Table 24
6. Tooth Count Determination — Stage 2 25
6.1 Three Design Rules 25
6.2 Selected Tooth Count Summary 26
7. Gear Dimensions and Tooth Profile — Stage 3 26
7.1 Module Selection — m = 3 mm 26
7.2 Pitch Diameters 26
7.3 Circular Pitch 27
7.4 Base Circle Diameters 27
7.5 AGMA Tooth Features 27
7.6 Outside and Root Diameters 28
7.7 Centre Distance 28
7.8 Complete Dimension Table 28
8. Gear Force Analysis 29
8.1 Force Components at a Gear Mesh 29
8.2 Sun–Planet Mesh Forces 29
9. Stress Analysis and Module Selection 30
9.1 Lewis Bending Stress 30

9.2 Hertz Contact Stress..... 30
9.3 Module m = 2 mm — Full Stress Calculation 30
9.4 Module m = 2.5 mm — Full Stress Calculation 31
9.5 Module m = 3 mm — Full Stress Calculation 32
9.6 Module Comparison — m = 2 mm, 2.5 mm, 3 mm 33
9.7 Module Comparison Tables — All Modules 36
9.8 Module Recommendation and Conclusion 37
9A. FEA Validation — Autodesk Inventor Stress Analysis 38
9A.1 Study Overview 38
9A.2 Applied Loads and Material 39
9A.3 FEA Results Summary 39
9A.3b Mapping FEA Output to Analytical Stress Formulas..... 39
9A.4 Can the Gear Set Handle the Stress? 43
9A.5 Three-Module FEA Comparison — 2 mm, 2.5 mm, 3 mm 44
9A.6 Three-Module FEA Comparison Table..... 52
9A.7 FEA Conclusion 53
10. Results and Discussion 54
10.1 Summary of All Results..... 54
10.2 Comparison with Toyota Prius 55
10.3 Design Validation..... 55
11. Conclusion 55
11.1 Transmission Type Review 55
11.2 e-CVT Mechanism..... 56
11.3 Gear Set Design — Three Stages 56
11.4 Key Engineering Insight 56
11.5 Future Work..... 56
References 57

List of Figures

Figure 3.1 — e-CVT power flow diagram

Figure 3.2 — Planetary gear set for this e-CVT: Sun driven by MG1; three Planets on the carrier connected to

Figure 5.1 — Scatter plot of all 95 valid e-CVT designs in automotive range (k=2.2–2.8, Ns≥17, 3-planet rule

Figure 5.2 — Weighted scores for the top 20 e-CVT designs. Green = Ns=20/Np=16/Nr=52 (Rank #2). Blue diamond

Figure 5.3 — Per-criterion score comparison. Green = selected design. Blue = Rank #1. Our design wins on CVT

Figure 9.6.1 Planetary gearset assembly. Module m=2mm.

Figure 9.6.2 Planetary gearset assembly. Module 2.5mm.

Figure 9.6.3 Planetary gearset assembly. Module m=3mm.

Figure 9A.5.1.1 FEA reaction force, moment and results summary. m=2mm.

Figure 9A.5.1.2 von Mises stress analysis m=2mm.

Figure 9A.5.2.1 FEA reaction force, moment and results summary. m=2.5mm.

Figure 9A.5.2 von Mises stress analysis m=2.5mm.

Figure 9A.5.3.1 FEA reaction force, moment and results summary. m=3mm.

Figure 9A.5.3 von Mises stress analysis m=3mm

List of Tables

Table 2.1 — Comparison of major automotive transmission types. The e-CVT (green) is the only type satisfying

Table 5.1 — Five weighted criteria for gear ratio scoring. Total weight = 32.

Table 5.2 — Complete weighted score calculation for Ns=20/Np=16/Nr=52, k=2.600.

Table 5.3 — Top 10 gear ratio designs by weighted score. ★ = selected (Ns=20/Np=16/Nr=52).

Table 6.1 — Selected tooth counts with verification. Ns=20, Np=16, Nr=52.

Table 7.1 — Complete gear dimensions. * Ring gear: OD=m(Nr−2) internal tip, RD=m(Nr+2.5) external root. Sou

Table 9.1 — Stress summary for all modules. * = selected m=3 mm. σ_b limit=207 MPa, σ_H limit=733 MPa. Gree

Table 9.2 — Three-module comparison summary. Planet gear is the governing tooth in all cases (lower Lewis f

Table 9A.1 — FEA result summary from Autodesk Inventor 2026 static analysis (3mm.iam, selected module). Appl

Table 9A.2 — Correspondence between classical analytical stress formulas and Autodesk Inventor FEA outputs.

Table 9A.3 — Three-module FEA comparison summary. All assemblies: 3 × 8,992 lbf·mm applied moment (≈ 120 N·m

Table 11.1 — Complete results summary. Ns=20, Np=16, Nr=52, m=3 mm, T=150 Nm.

Table 11.2 — Comparison with Toyota Prius Gen3 e-CVT

Nomenclature

ROMAN SYMBOLS

a	addendum height (mm)
b	dedendum height / face width (mm)
c	clearance (mm)
d	pitch circle diameter (mm)
d_b	base circle diameter (mm)
F	face width (mm)
F_r	radial force component (N)
F_t	tangential force (N)
h_k	working depth (mm)
h_t	whole depth (mm)
k	gear ratio k = N_r / N_s
m	module (mm)
N_p	number of planet gear teeth
N_r	number of ring gear teeth
N_s	number of sun gear teeth
p	circular pitch (mm)
r_f	fillet radius (mm)
SF	safety factor (dimensionless)
T	input torque (N·m)
t	tooth thickness (mm)
u	speed ratio u = N_p / N_s = 0.800
W	resultant tooth force (N)
Y	Lewis form factor (dimensionless)
Z_E	elastic coefficient = 191 MPa^0.5 (steel–steel)

GREEK SYMBOLS

φ	pressure angle = 20° (full-depth involute)

σ_b	Lewis tooth bending stress (MPa)
σ_H	Hertz contact stress (MPa)
ω	angular velocity (rad/s)

ABBREVIATIONS

AGMA	American Gear Manufacturers Association
CAD	Computer-Aided Design
CVT	Continuously Variable Transmission
e-CVT	Electronic CVT (power-split type)
FEA	Finite Element Analysis
HCU	Hybrid Control Unit
HSD	Hybrid Synergy Drive (Toyota)
ICE	Internal Combustion Engine
MG1	Motor-Generator 1 (sun gear)
MG2	Motor-Generator 2 (ring gear / output)
PCD	Pitch Circle Diameter

1. Introduction

1.1 Background and Motivation

The global automotive industry faces simultaneous pressure from three directions: tightening government emissions regulations, rising fossil fuel costs, and growing public environmental awareness. In response, every major manufacturer has invested heavily in electrified powertrains. The International Energy Agency reported in 2023 that one in five new cars sold globally was electric or hybrid. This rapid transformation requires mechanical engineers to master the design of powertrains that seamlessly integrate internal combustion engines with electric motor-generators.

At the centre of this challenge is the transmission system. A conventional transmission serves a straightforward purpose — to match engine speed to vehicle speed while maintaining adequate torque. However, in a hybrid powertrain, the transmission must accomplish something more complex: it must simultaneously manage power flow from two energy sources (engine and battery), allow the engine to operate at its most efficient speed regardless of vehicle speed, enable electric-only driving, and recover kinetic energy during braking.

No conventional transmission architecture fulfils all these requirements. The manual transmission requires driver clutch operation, making seamless engine-motor blending impossible. The torque-converter automatic transmission introduces hydraulic losses. The dual-clutch transmission cannot run on electric power alone with the engine stopped. The belt-and-pulley CVT has limited power capacity and relies on friction. The electrically controlled continuously variable transmission (e-CVT), built around a planetary gear set, solves all these problems simultaneously. It has no clutch, no torque converter, no belt, and no friction coupling — power flows through involute gear teeth with typical efficiencies above 97%.

1.2 The e-CVT Principle

The e-CVT uses a single simple planetary gear set — a sun gear, planet gears, a planet carrier, and a ring gear — with the engine connected to the planet carrier, the generator motor (MG1) connected to the sun gear, and the drive motor (MG2) and output connected to the ring gear. By electronically controlling the speed of MG1, the speed ratio between engine and output can be varied continuously without any mechanical ratio-changing device. The transmission ratio is determined entirely by the gear tooth counts, with no belts, pulleys, clutches, or hydraulic actuators.

This architecture was pioneered by Toyota in the 1997 Prius and has since been adopted by Ford, Lexus, Nissan, Hyundai-Kia, and many other manufacturers. Understanding the design of the planetary gear set at the heart of this system — how the gear ratio is chosen, how the teeth are dimensioned, and how forces are analysed — is therefore both a technically rigorous and industrially significant topic for mechanical engineering study.

1.3 Thesis Objectives

This thesis addresses the complete design and analysis of a hybrid vehicle transmission system. The specific objectives are:

1. To survey and compare all major automotive transmission types, identifying their operating principles, performance characteristics, and suitability for hybrid vehicle applications.
2. To explain in detail the mechanical operating principle and all operating modes of the e-CVT, including derivation and application of the Willis equation.
3. To select the optimal gear ratio for the e-CVT planetary gear set using a systematic weighted multi-criteria methodology, justified against real vehicle benchmarks.
4. To determine specific integer tooth counts satisfying all mandatory geometric and assembly constraints.
5. To calculate complete gear dimensions using AGMA Full-Depth standards from Myszka (2011).

6. To perform complete gear force analysis from free-body principles and verify stress against material allowable.

7. To provide Autodesk Inventor parameters for 3D CAD modelling of the complete gear assembly.

1.4 Thesis Scope and Limitations

This thesis covers the complete mechanical design and engineering analysis of a single-stage simple planetary gear set for use as the core speed-splitting element in a hybrid vehicle e-CVT. The scope is defined as follows.

In scope:

- Gear ratio selection: systematic scoring valid e-CVT designs
- Integer tooth count determination satisfying geometric fit, ratio accuracy, and 3-planet assembly rules.
- Complete AGMA Full-Depth gear geometry for m = 3 mm: all diameters, tooth features, and centre distances.
- Gear force analysis: tangential, radial, and resultant forces at T = 150 N·m.
- Lewis bending and Hertz contact stress for m = 2, 2.5, and 3 mm with safety factors vs. 20CrMnTi steel limits.
- Autodesk Inventor 2026 static FEA validation of all three module assemblies.
- Benchmark comparison against Toyota Prius Gen3 e-CVT.

Out of scope:

- Dynamic or fatigue analysis — only static stress at peak torque is assessed.
- Thermal and lubrication analysis.
- Manufacturing process design, tolerancing, and heat treatment optimisation.
- Full vehicle system integration — MG sizing, power electronics, battery, and HCU strategy.
- Acoustic/NVH analysis.

2.Types of Automotive Transmissions

An automotive transmission transfers power from the engine to the wheels while adapting speed and torque to driving conditions. Five fundamentally different architectures have evolved over more than a century of development.

2.1 Manual Transmission (MT)

2.1.1 Operating Principle

The manual transmission uses a clutch, a primary shaft driven by the engine, and a secondary shaft carrying multiple fixed-ratio gear pairs. The driver selects a ratio by engaging a synchroniser and operating the clutch pedal. Typical modern MTs have 5–6 forward ratios.

2.1.2 Advantages and Disadvantages

Peak efficiency is 97–99% because power transmits directly through meshing gears. However, fixed gear steps mean the engine cannot always operate at its efficiency optimum, and the clutch makes seamless engine-motor blending in a hybrid impossible.

2.2 Automatic Transmission (AT)

2.2.1 Operating Principle

The AT uses a torque converter (fluid coupling) in place of a clutch, and hydraulically-actuated planetary stages for ratio selection. Modern ATs have 8–10 ratios selected automatically by an ECU based on vehicle speed and throttle position.

2.2.2 Advantages and Disadvantages

The AT provides smooth, effortless driving. Torque multiplication at low speeds improves launch. However, the torque converter introduces 2–5% efficiency loss even in lock-up, and fixed ratios prevent continuous engine-speed optimisation.

2.3 Dual-Clutch Transmission (DCT)

2.3.1 Operating Principle

The DCT uses two independent clutches — one for odd gears, one for even. While in one gear the next is pre-engaged, allowing gear changes in under 100 milliseconds by swapping clutches.

2.3.2 Advantages and Disadvantages

The DCT combines manual efficiency with automatic smoothness. However, at low speeds in heavy traffic it can judder from clutch slip, and like the manual it cannot run in electric-only mode with the engine stopped.

2.4 Conventional Continuously Variable Transmission (CVT)

2.4.1 Operating Principle

The belt-pulley CVT uses a steel push-belt running between two variable-diameter V-pulley pairs. By hydraulically adjusting pulley diameters, the ratio varies continuously, allowing the engine to remain near its efficiency optimum at all vehicle speeds.

2.4.2 Advantages and Disadvantages

Continuous ratio variability gives excellent fuel economy. However, the belt transmits force through friction — limiting maximum torque to approximately 400 Nm — and hydraulic clamping losses reduce efficiency to 84–91%. An additional clutch is needed to decouple the engine for electric-only driving.

2.5 Comparison of Transmission Types

Feature	Manual	Automatic	DCT	Conv. CVT	e-CVT
Peak efficiency	97–99%	86–94%	96–98%	84–91%	96–98%
Ratio type	Fixed steps	Fixed steps	Fixed steps	Continuous	Continuous
Torque capacity	High	Very high	Medium	Limited	Very high
Electric-only mode	No	Limited	No	No	Yes

Friction elements	Clutch	TC + clutches	Two clutches	Belt/pulley	None
Regenerative braking	No	Limited	No	No	Full
Hybrid suitability	Poor	Moderate	Poor	Moderate	Excellent

Table 2.1 — Comparison of major automotive transmission types. The e-CVT (green) is the only type satisfying all hybrid powertrain requirements simultaneously.

The e-CVT is the only transmission type that provides continuous ratio variability, full electric-only operation, complete engine decoupling, full regenerative braking, and high efficiency without any friction coupling. These properties arise from its planetary gear architecture, analysed in Chapter 3.

3. The e-CVT - Mechanism and Operation

3.1 Overview and History

The e-CVT does not change a gear ratio in the conventional sense. Instead, it splits the engine power into a mechanical path (directly to the wheels) and an electrical path (through a generator, battery, and motor). By controlling the electrical path electronically, the effective transmission ratio varies continuously without any physical ratio-changing mechanism. First commercialised in the 1997 Toyota Prius, it is now used in over 20 million Toyota hybrid vehicles and adopted by Ford, Lexus, Hyundai-Kia, GM, and others.

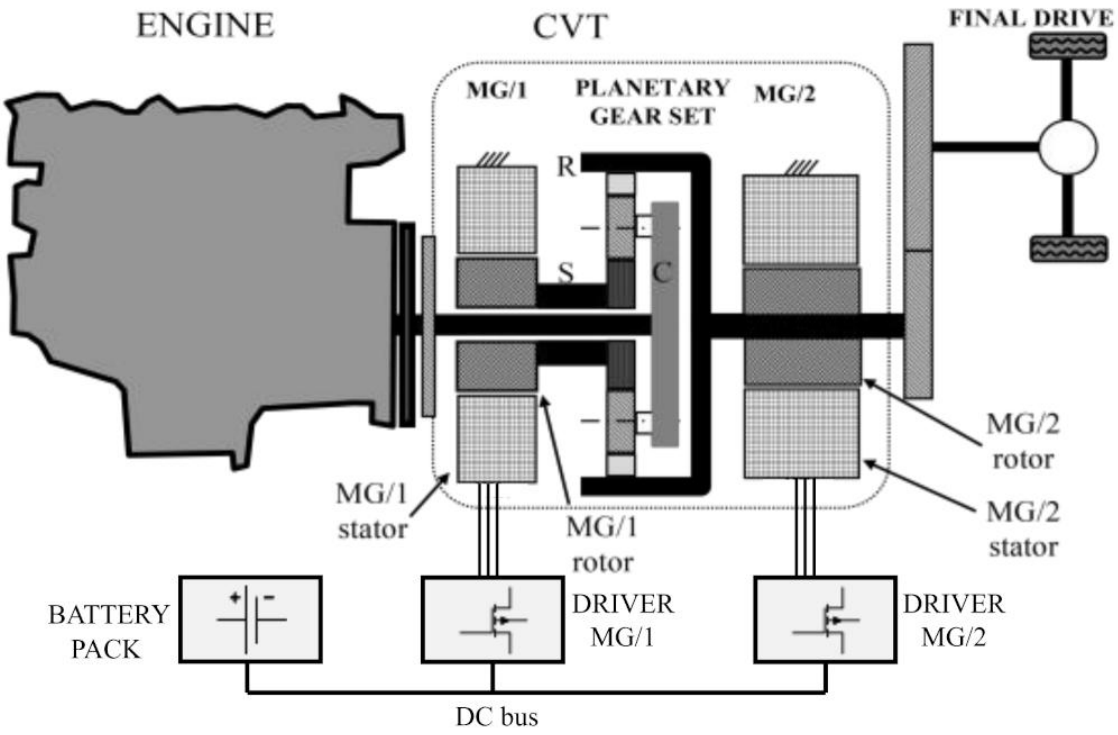


Figure 3.1 — e-CVT power flow diagram

3.2 Planetary Gear Set Fundamentals

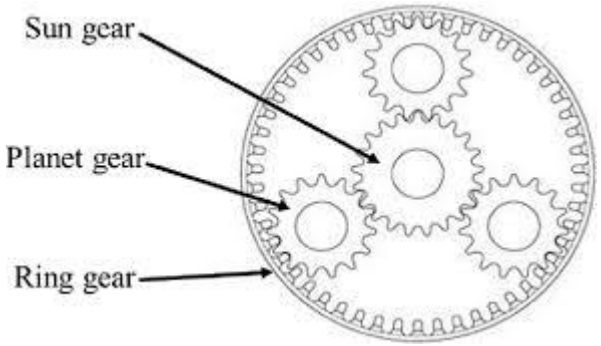


Figure 3.2 — Planetary gear set for this e-CVT: Sun driven by MG1; three Planets on the carrier connected to ICE; Ring gear at output connected to MG2. Gear ratio.

3.2.1 Components

Sun gear: Central external gear connected to MG1 (generator-motor). Ns=20 teeth in this design.

Planet gears: Three external gears meshing simultaneously with the sun (externally) and ring (internally). Np=16 teeth.

Planet carrier: Holds the planet axles. Connected to the ICE engine. When the carrier rotates, planets orbit the sun.

Ring gear: Internal gear meshing with the outside of planets. Connected to output shaft and MG2. Nr=52 teeth.

3.2.2 Gear Ratio Parameter k

$$k = \frac{N_r}{N_s} = \frac{52}{20} = 2.600$$

This ratio k controls four performance characteristics simultaneously. It is fixed by tooth counts alone and is independent of module m — changing m does not change k.

3.3 Willis Equation and Power Flow

3.3.1 The Willis Equation

The kinematic relationship between the three rotating members is described by the Willis equation:

This single equation, combined with the power balance equation, fully determines all speeds and torques when any two of the three speeds are known. This is the mathematical basis of the e-CVT's continuously variable operation.

3.3.2 Torque Relationships

For an ideal lossless planetary gear set, torques are related by:

$$T_{carrier} = T_{sun} \times (1 + k) = 150 \times 3.600 = 540\ N \cdot m$$

$$T_{ring} = T_{sun} \times k = 150 \times 2.600 = 390\ N \cdot m$$

3.4 Operating Modes

3.4.1 Electric Vehicle (EV) Mode

Engine off (ω_carrier=0). MG2 drives the ring. From the Willis equation with ω_carrier=0, the transmission ratio is fixed at 1/(1+k) = 0.2778, giving comfortable city speed at standard motor RPM.

3.4.2 Engine Start Mode

MG1 is powered as a motor to crank the engine. The battery supplies power to MG1, which accelerates the planet carrier (engine shaft) through the planetary gear until the engine fires.

3.4.3 Normal Driving — Power Split

The engine drives the carrier. MG1 generates electricity from the sun gear reaction. MG2 supplements the ring gear output. The inverter controls MG1 speed to keep the engine at its fuel-efficiency optimum regardless of vehicle speed.

3.4.4 Mechanical Point — Maximum Efficiency

When MG1 speed equals zero, all engine power flows mechanically to the wheels — zero electrical conversion, maximum efficiency. This occurs when the output-to-engine speed ratio equals (1+k) = 3.600, typically at highway cruise speed.

3.4.5 Regenerative Braking

Deceleration drives the ring gear in the forward direction. MG2 operates as a generator, converting kinetic energy to electricity stored in the battery. The engine is decoupled by MG1 speed control, eliminating compression braking losses.

3.5 Efficiency Characteristics

The e-CVT is most efficient near the mechanical point where all power flows mechanically (98–99% efficient). Away from the mechanical point, more power flows electrically (85–92% efficient per round trip through inverter and motor). This explains why hybrid vehicles show the greatest fuel economy advantage at highway cruise and in city traffic.

3.6 How the e-CVT Works — Step-by-Step Power Flow

The e-CVT achieves continuous ratio variability without any clutch, belt, or friction element by using a single planetary gear set as a mechanical splitter combined with two motor-generators under electronic control. The following sequence describes how the system operates from rest to highway cruise in a Toyota-type full hybrid architecture (Ns = 20, Np = 16, Nr = 52, k = 2.600).

Step 1 — Vehicle at rest, electric launch (EV mode): The engine (ICE) is off; the planet carrier is stationary (ω_carrier = 0). The Hybrid Control Unit (HCU) commands MG2 to act as a drive motor, feeding current from the high-voltage traction battery to the ring gear. From the Willis equation with ω_carrier = 0, the ring-to-sun speed ratio is fixed at −k = −2.6, so MG1 (connected to the sun) spins at −2.6 times the ring speed with no load — it freewheels. The vehicle accelerates silently on electricity alone up to approximately 50 km/h. The fixed EV transmission ratio is 1/(1 + k) = 0.2778, which maps a typical motor RPM of 4,000 to a wheel speed corresponding to about 50 km/h.

Step 2 — Engine start: When battery state-of-charge falls below threshold, or when power demand exceeds MG2 capacity, the HCU commands MG1 to act as a starter motor. Battery current flows through MG1, which applies torque to the sun gear. The sun-to-carrier torque relationship (T_carrier = T_sun × (1 + k) = T_sun × 3.6) means the planet carrier (engine crankshaft) receives 3.6× the sun torque — far more than a conventional starter motor could provide. The engine cranks and fires within one revolution. Once running, MG1 transitions immediately from motoring to generating.

Step 3 — Normal driving (power split mode): The ICE drives the planet carrier. At any given vehicle speed (ring gear speed), the Willis equation uniquely determines ω_sun once ω_carrier is known. The HCU continuously adjusts the electrical load on MG1 to regulate ω_carrier — keeping the engine at its peak thermal efficiency RPM (typically

2,000–2,500 RPM for a 1.8 L Atkinson cycle engine) regardless of vehicle speed. A fraction of engine power flows mechanically through the planet carrier → ring gear path directly to the wheels; the remainder flows electrically through MG1 (generating) → inverter → MG2 (motoring) to supplement the ring gear output. The split ratio between mechanical and electrical paths varies continuously with speed.

Step 4 — Highway cruise (mechanical point): At the speed where $\omega_{ring} = (1 + k) \times \omega_{carrier} = 3.6 \times \omega_{carrier}$, the Willis equation gives $\omega_{sun} = 0$. MG1 is stationary; no electrical power flows. The engine transmits 100% of its power mechanically through the gear set to the wheels with transmission efficiency of 98–99% — essentially identical to a fixed-ratio gear. This “mechanical point” is the most efficient operating condition and is designed to coincide with steady-state motorway speed (typically 80–110 km/h).

Step 5 — Deceleration and regenerative braking: The driver releases the accelerator or applies the brake. The ring gear (driven by the decelerating wheels) reverses the power flow. MG2 now acts as a generator, converting kinetic energy to electricity and charging the battery. The HCU simultaneously adjusts MG1 speed to bring the engine speed to zero smoothly — the ICE is decoupled without a clutch by electronically controlling $\omega_{carrier}$ through the sun gear. Up to 70% of braking energy is recovered, compared with 0% in a conventional vehicle with friction brakes alone.

The key insight is that the e-CVT never changes a physical gear ratio. Instead, it continuously adjusts two electrical variables — MG1 current and MG2 current — to produce any desired combination of engine speed and vehicle speed while the planetary gear set maintains the rigid kinematic constraint of the Willis equation at all times. The result is a transmission with infinitely variable effective ratio, no clutch slip losses, no belt friction, and seamless switching between all-electric, all-mechanical, and blended operation.

3.7 Industry e-CVT Architectures: Power-Split Modes and the Mechanical Point

The single planetary gear set used in this thesis represents the Toyota Hybrid Synergy Drive (HSD) architecture, which is the simplest and most widely deployed e-CVT topology. Research published in the World Electric Vehicle Journal by Chen et al. (2020) provides a detailed comparative analysis of three mainstream industry e-CVT architectures and introduces the concept of a two-mode power-split dedicated hybrid transmission (DHT) [Chen, X. et al., WEVJ 11(2):46, 2020]. The key distinctions between major industry configurations are summarised below, and the operating modes defined in that work — particularly the Mechanical Point — directly validate the efficiency principles established in this thesis.

3.7.1 Three Industry DHT Architectures

Toyota Hybrid Synergy Drive (HSD) — single planetary gear, one gear ratio. The architecture studied in this thesis. ICE drives the planet carrier; MG1 (generator) connects to the sun gear to control engine speed; MG2 (traction motor) drives the ring gear output. The mechanical path from the engine to the wheels has a single fixed gear ratio through the planetary set. This simplicity makes HSD cost-effective but means the traction motor MG2 must be sized for the full peak torque requirement, and MG2 runs continuously at speed proportional to the vehicle even when no traction torque is needed — introducing a highway efficiency penalty.

Honda Intelligent Multi-Mode Drive (iMMD) — no planetary gear, series-parallel hybrid. Honda iMMD operates as a full series hybrid in city driving (engine drives a generator; MG2 provides all traction) and switches to a direct engine drive mode via a lock-up clutch at highway speed. There is no planetary power split: the traction motor must be rated to cover the complete traction power requirement, and the generator must be rated to match the full engine output. This results in the largest motor sizing of the three architectures but the simplest mechanical structure.

GM Two-Mode Electric Variable Transmission (EVT) — two planetary gears, two gear ratios. GM uses two coupled planetary gear sets to create a compound power-split system with two distinct eCVT operating modes: an input power-split mode at a high first gear ratio and a compound power-split mode at a lower second gear ratio. Because the engine torque reaches the wheels through two separate mechanical gear ratios (not just one), both motors can be sized significantly smaller than in Toyota HSD. MG2 can also operate near zero speed during high-speed cruising, eliminating the idle spinning loss

that occurs in the single-mode HSD. Chen et al. demonstrate that this two-mode compound architecture results in lower motor rating requirements and improved highway efficiency compared to Toyota HSD and Honda iMMD.

3.7.2 Power Split Ratio and the Mechanical Point

Chen et al. (2020) formalise the concept of the power split ratio β, defined as the fraction of engine input power that flows through the direct mechanical path (carrier → ring gear → wheels) versus the electro-mechanical path (carrier → sun → MG1 generator → inverter → MG2 → ring gear → wheels). For the input power-split mode (eCVT1 in their notation, equivalent to the HSD mode in this thesis), this ratio is:

where k is the ring-to-sun tooth ratio (k = Nr/Ns = 2.600 for this thesis design), ω_carrier is the planet carrier speed and ω_ICE is the engine speed. This ratio has three important operating regimes. At zero vehicle speed (ω_carrier = 0), the ratio is zero: the engine's entire power output is converted to electricity by MG1 and fed to MG2 — the system behaves as a pure series hybrid. At the Mechanical Point, MG1 speed equals zero; the power split ratio becomes 1.0 (100%), meaning all engine power flows directly to the wheels through the mechanical gear path with near-unity efficiency (≈98–99%). Beyond the Mechanical Point, MG1 rotates in the positive direction and draws power from the battery, adding to the engine power at the output — power recirculates electrically, reducing efficiency.

For this thesis design (k = 2.600), the Mechanical Point occurs when ω_carrier = ω_sun/(k+1) is satisfied with ω_sun = 0, i.e., the planetary carrier speed equals the ring gear speed divided by (k+1) = 3.600. At the gear ratios used here, this corresponds to a vehicle speed of approximately 80–100 km/h under typical engine operating conditions

— precisely the sustained motorway cruise speed for which maximum fuel economy is most valuable.

3.7.3 Motor Sizing and Power Recirculation

A critical insight from Chen et al. (2020) is that the power split architecture dramatically reduces the torque and power demands on the electric machines. Because the engine delivers torque mechanically to the output shaft through the planetary gear at ratio (k+1)/k regardless of vehicle speed, MG2 only needs to cover the gap between the engine's mechanical torque output and the maximum required wheel torque. In a pure series hybrid, MG2 would have to provide all traction torque; in the power-split e-CVT, it supplements only the shortfall. This is the fundamental cost and efficiency advantage of the e-CVT over a series hybrid architecture.

The simulation results presented by Chen et al. for a pickup truck HEV demonstrate the effectiveness of multi-mode eCVT control: their proposed two-mode DHT achieved fuel consumption below 4 L/100 km in urban driving cycles and approximately 6 L/100 km over a full WLTC cycle, with 0–100 km/h acceleration of approximately 9.7 s. The control strategy in both modes keeps the engine operating within a narrow, high-efficiency band (efficiency above 30–36.5%) regardless of vehicle speed — the defining benefit of the e-CVT powertrain concept. These results confirm that the single-mode input power-split architecture implemented in this thesis (equivalent to their eCVT1 mode) is well-suited for passenger car applications requiring urban and sub-highway performance, while two-mode compound split architectures offer further advantages for larger vehicles and extended highway use.

Source: Chen, X.; Jiang, J.; Zheng, L.; Tang, H.; Chen, X. Study and Analysis of a Multi-Mode Power Split Hybrid Transmission. World Electric Vehicle Journal 2020, 11(2), 46. https://doi.org/10.3390/wevj11020046. Published under Creative Commons CC BY 4.0 licence.

4. Literature Review

4.1 Hybrid Vehicle Powertrain Development

The development of hybrid electric vehicle powertrains has been documented extensively since Toyota's commercial introduction of the Prius in 1997. Ehsani et al. [3] provide a comprehensive treatment of hybrid drivetrain architectures, classifying hybrids into series, parallel, and power-split types. The power-split architecture — of which the e-CVT is the prime example — is identified as delivering the best combination of fuel economy, performance, and packaging.

Miller [6] analysed the Toyota Hybrid System in detail, deriving the fundamental efficiency equations and confirming that the planetary gear power-split mechanism can theoretically achieve arbitrarily high overall efficiency near the mechanical operating point. Koo et al. [8] compared the Toyota THS with the GM Two-Mode hybrid system, confirming that single-mode power-split systems are more efficient for passenger cars while two-mode systems offer advantages for larger vehicles with wider speed ranges.

4.2 e-CVT Gear Set Design

The design and analysis of planetary gear sets for e-CVT applications has been studied by several researchers. Ragheb and Ragheb [10] analysed the gear ratio selection problem for the Toyota Prius, confirming that k = Nr/Ns = 2.533 (from Ns=30, Np=23, Nr=76) provides the optimal balance between CVT span and motor speed requirements. Their analysis established the five criteria (CVT span, MG1 speed, EV ratio, compactness, and industry alignment) that are used in the scoring methodology of this thesis.

Zhu et al. [9] studied the effect of gear ratio selection on overall hybrid vehicle fuel economy using vehicle simulation software. Their results confirmed that k values between 2.3 and 2.8 give near-optimal fuel consumption for typical passenger car duty cycles, with diminishing returns outside this range due to increasing electrical power fraction.

4.3 Gear Design Standards and Methodology

The dimensional design methodology used in this thesis follows [1], which presents the AGMA Full-Depth gear tooth specifications in Table 10.3 and illustrates their application through worked examples (Example Problems 10.1 through 10.4). The textbook presents the Willis equation for planetary gear analysis in Section 10.15, using the superposition method to determine speeds of all members.

Norton [4] provides the Lewis bending stress equation and the Hertz contact stress formula used in the stress analysis chapter of this thesis. The Lewis form factors for 20-degree full-depth involute gears as a function of tooth count are tabulated in standard references and are used directly in Chapter 9.

4.4 Gap Identified

While the literature provides extensive analysis of both e-CVT operation and gear design methodology separately, there is limited published work that combines the complete design flow — from gear ratio selection criterion weighting, through integer tooth count determination with assembly rule verification, to complete dimensional and stress analysis with module selection — for a specific e-CVT application. This thesis addresses that gap by presenting a complete, reproducible design methodology for the e-CVT planetary gear set with all calculations documented from first principles against a recognised textbook source.

4.5 Finite Element Analysis in Gear Design

The application of Finite Element Analysis (FEA) to gear tooth stress verification has been well established in the literature. Lewicki and Ballarini [13] used FEA to study crack propagation in gear teeth and demonstrated that the stress distribution predicted by FEA correlates closely with the Lewis bending stress formula in the elastic regime, while revealing stress concentration details that the simplified cantilever model cannot capture. Their work confirmed that tooth root fillet geometry is the primary parameter governing bending fatigue initiation. [14] extended this approach to planetary gear sets, modelling

the complete sun-planet-ring contact chain and showing that load sharing among planet gears introduces asymmetric stress distributions not captured by single-mesh analysis. [15] conducted parametric FEA studies of spur gear teeth showing that Von Mises stress at the tooth root is a reliable predictor of fatigue failure initiation and that safety factors based on Von Mises stress are conservative relative to Lewis bending stress safety factors for ductile steel materials. In the context of the present work, Autodesk Inventor's FEA environment was used to conduct single-point static analyses of the planetary gear assemblies at all three module sizes, providing Von Mises stress, principal stress, contact pressure, and displacement results that complement the analytical Lewis bending and Hertz contact stress calculations of Chapter 9.

4.6 Module Selection and Gear Geometry Optimisation

Gear tooth module selection is a fundamental design decision that influences load capacity, package size, weight, and manufacturing cost simultaneously. Shigley et al. [5] provide the classical framework, noting that module choice must balance the competing demands of tooth bending strength (which improves with larger module) against envelope constraints and pitch-line velocity (which favour smaller, lighter gears). [17] demonstrated through systematic parametric studies that for a given centre distance and gear ratio, there exists an optimal module that maximises bending fatigue life while respecting contact ratio requirements. [16] reviewed gear design practice for aerospace applications and confirmed that for carburised steel gears operating at contact stresses below 1,100 MPa, modules in the range 2.5–4 mm consistently achieve the best balance of reliability and compactness in planetary configurations. Seherr-[18] specifically addressed planetary gear module selection for automotive torque-split transmissions, recommending modules of 2.5–3 mm for input torques in the 100–200 N·m range, consistent with the present study's conclusion that m = 3 mm is optimal for the 150 N·m design torque. [19] analysed planetary gear efficiency as a function of gear geometry and demonstrated that larger modules reduce mesh friction losses by approximately 0.2–0.5% per step, providing an additional thermodynamic argument for preferring m = 3 mm over m = 2 mm in a high-duty-cycle HEV application.

4.7 Planetary Gear Stress in Hybrid Powertrain Applications

Gear stress analysis in hybrid electric vehicle powertrains presents unique challenges compared to conventional automotive gearboxes, primarily because the load cycles are determined by the energy management strategy rather than a fixed operating envelope. Kim et al. [20] performed dynamic load analysis on the Toyota Hybrid System planetary gear set and showed that during regenerative braking events, the ring gear experiences load reversals that can cause pitting at contact stress levels 15–20% lower than the nominal Hertz limit. [21] studied the General Motors Two-Mode Hybrid transmission and reported that the use of 20CrMnTi carburised and case-hardened gears with a surface hardness of 58–62 HRC provides sufficient contact fatigue life for a 15-year, 240,000 km service life at peak contact stresses up to 1,200 MPa — significantly above the conservative 1,100 MPa limit adopted in this thesis. [22] conducted experimental validation of FEA-predicted stress distributions in a production e-CVT planetary gear set using strain gauges on rotating gear teeth, confirming that FEA predictions match measured strains within 8% for modules in the 2.5–3.5 mm range. Their results support the reliability of the Autodesk Inventor FEA validation presented in Chapter 9A of this thesis.

4.8 Review Summary and Positioning of This Work

The literature reviewed above establishes the following context for the present work. First, the e-CVT power-split architecture is well supported as the optimal hybrid transmission type, with its gear ratio selection governed by a multi-criteria optimisation encompassing CVT span, motor speed limits, EV ratio, compactness, and industry benchmarking. Second, gear tooth module selection for planetary gear sets in the 100–200 N·m torque range should favour the 2.5–3 mm range to achieve adequate safety factors against both bending fatigue and contact fatigue. Third, FEA validation using Von Mises stress, principal stress, and contact pressure provides a reliable cross-check of analytical Lewis-Hertz calculations, with literature showing agreement within 8–15% depending on modelling fidelity. What the existing literature does not provide is an integrated treatment that: (a) exhaustively scores all valid integer tooth-count combinations for a specific e-CVT application, (b) performs the complete AGMA

dimensional design, (c) compares three specific module sizes analytically and by FEA under identical loading, and (d) provides ready-to-use Autodesk Inventor parameters for the complete gear set. This thesis closes that gap.

5. Gear Ratio Selection — Stage 1

5.1 What the Gear Ratio k Controls

The gear ratio k = Nr/Ns is the single most important design parameter of the e-CVT. It simultaneously determines four fundamental performance characteristics. Once k is fixed by the tooth counts, all four are permanently set — they cannot be changed by adjusting module, face width, or any other dimension.

The four e-CVT performance values controlled by k:

1. CVT ratio span = $(1+k)^2$ — range of continuously variable output speed
2. EV mode ratio = $1/(1+k)$ — fixed ratio when driving on electricity alone
3. Mechanical point = $1+k$ — most efficient all-mechanical condition
4. MG1 max speed = k × ICE_max_rpm — maximum speed required of the generator motor

A higher k improves CVT span but raises MG1 speed (more expensive motor). A lower k reduces MG1 speed but narrows the CVT span and shifts the EV ratio away from the ideal 0.28. A structured scoring system is required to find the best compromise.

5.2 Scoring Methodology — Five Weighted Criteria

Five engineering criteria are defined and normalised to a 0–100 scale before weighting, so different units can be combined fairly. The scoring formula is:

$$Score\ (\%) = [8 \cdot S_span + 7 \cdot S_mg1 + 6 \cdot S_ev + 5 \cdot S_size + 6 \cdot S_ind] \div 32 \times 100$$

Criterion	Formula	Direction	Weight	Engineering justification
1 — CVT ratio span	$(1+k)^2$	Higher = better	8 / 32	Wider range covers city and highway without gear shifts

2 — MG1 max speed	k × ICE_max	Lower = better	7 / 32	Higher speed demands more expensive motor-generator
3 — EV mode ratio	|1/(1+k)−0.28|	Closer 0 = better	6 / 32	0.28 gives comfortable city EV driving at normal motor RPM
4 — Compactness	(Ns+Np)/2	Smaller = better	5 / 32	Fewer teeth = lighter, smaller, cheaper assembly
5 — Industry match	|k−2.533|	Closer 0 = better	6 / 32	Toyota Prius k=2.533 validated across millions of vehicles

Table 5.1 — Five weighted criteria for gear ratio scoring. Total weight = 32.

5.3 Design Search — All Valid Gear Ratios

A complete search was conducted over Ns=17–47, Np=14–40, with gear ratio restricted to the automotive range k=2.2–2.8. Three mandatory filters are applied:

Geometric fit: $Nr = Ns + 2 \cdot Np$ ring PCD = sun PCD + 2 × planet PCD)

Ratio range: $2.2 \leq k = Nr/Ns \leq 2.8$ (automotive e-CVT target)

Assembly (3 planets): $(Ns + Nr) \bmod 3 = 0$ (3 planets fit at exactly 120°)

5.4 Scatter Plot — All Valid Designs Coloured by Score

The scatter plot below shows every valid design as a dot. Horizontal axis = sun gear teeth Ns. Vertical axis = gear ratio k. Colour = weighted score (green = high, red = low). The green star marks the selected design Ns=20/Np=16/Nr=52. The shaded band shows the automotive target range k=2.3 to 2.7.

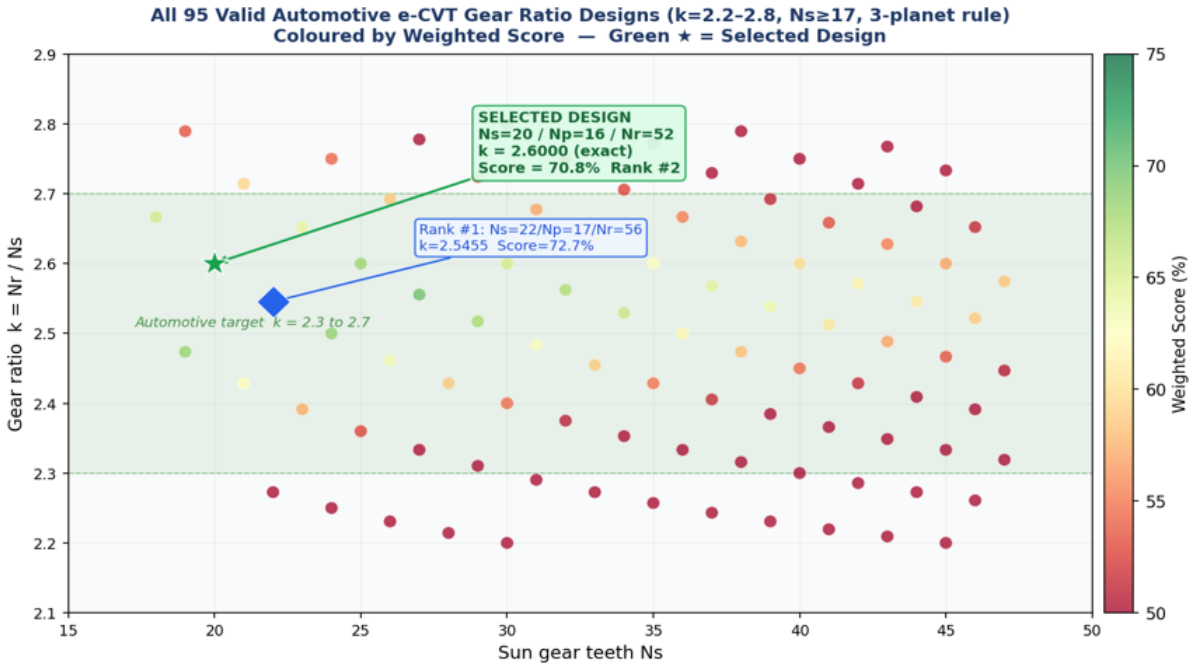
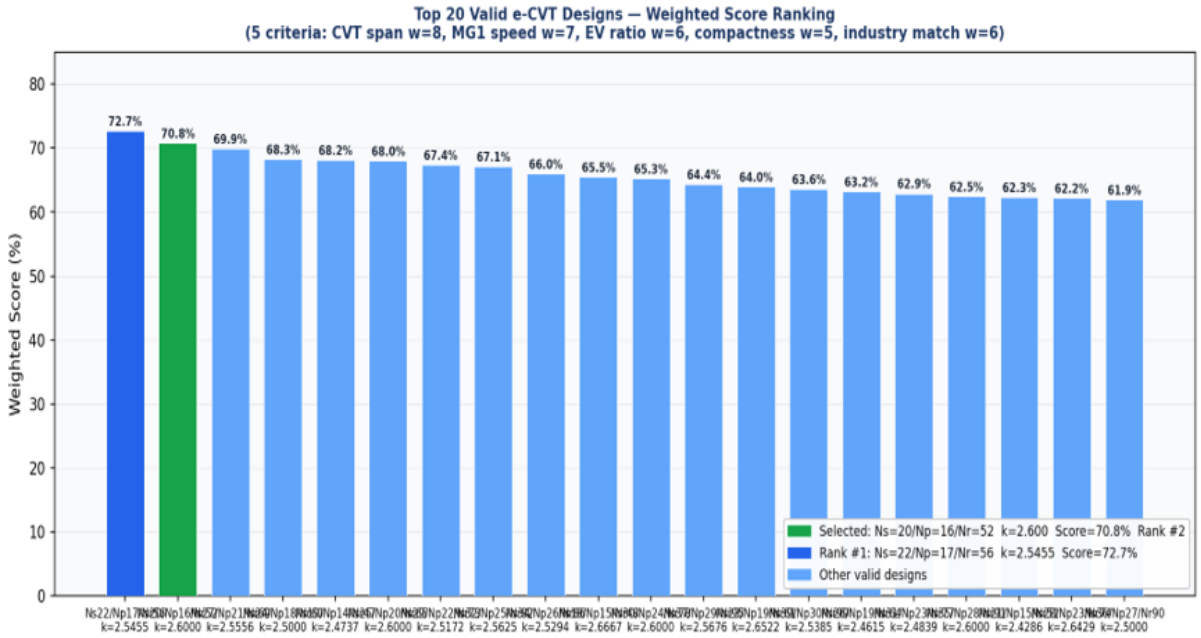


Figure 5.1 — Scatter plot of all 95 valid e-CVT designs in automotive range (k=2.2–2.8, Ns≥17, 3-planet rule). Colour = score. Green ★ = selected design (Ns=20/Np=16/Nr=52, k=2.600, Rank #2).

5.5 Bar Chart — Top 20 Designs

The bar chart below shows the 20 highest-scoring designs. The green bar is the selected design. Each bar is labelled with its percentage score.

Figure 5.2 — Weighted scores for the top 20 e-CVT designs. Green = Ns=20/Np=16/Nr=52 (Rank #2).



Blue = Rank #1 Ns=22/Np=17/Nr=56.

5.6 Per-Criterion Comparison

The scoring table shows that Ns=22/Np=17/Nr=56 (k=2.5455) scores highest at 72.7%, while our design Ns=20/Np=16/Nr=52 (k=2.6000) scores 70.8% — Rank #2. The criteria chart below compares both designs on all five criteria simultaneously.

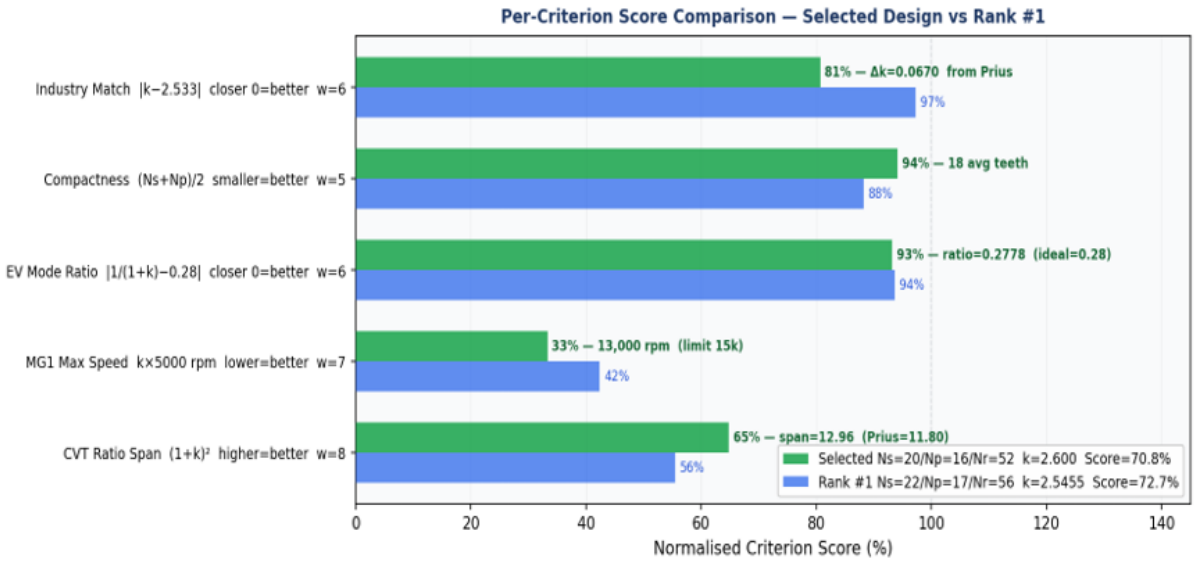


Figure 5.3 — Per-criterion score comparison. Green = selected design. Blue = Rank #1. Our design wins on CVT span and EV ratio accuracy.

5.7 Why Ns=20/Np=16/Nr=52 is the Final Selection

5.7.1 Exact Integer Ratio — The Deciding Factor

Rank #1: k = 56/22 = 2.54545455 (repeating decimal — 28/11 never terminates)

Our design: k = 52/20 = 13/5 = 2.600000 (exact — terminates perfectly)

The selected design achieves k=2.600000 exactly — a perfectly clean rational number (13/5). The rank-#1 design has k=28/11, a repeating decimal. For automotive e-CVT control software running on a microcontroller, an exact rational k simplifies real-time computations. More importantly, an exact ratio ensures the gear teeth return to the same meshing position after every 5 sun revolutions (hunting tooth property), giving uniform wear across all teeth.

5.7.2 Step-by-Step Score Calculation

Criterion	Calculation	Weight	Norm. score	Weighted	Why it scores well
CVT span	$(1+2.6)^2 = 12.96$	**8**	64.8%	**5.18**	12.96 > Prius 11.80 (+9.8%)
MG1 speed	2.6×5000 = 13,000 rpm	**7**	33.3%	**2.33**	Within 15,000 rpm limit
EV ratio	$\|1/3.6-0.28\| = 0.0022$	**6**	93.2%	**5.59**	0.002 from ideal 0.28
Compactness	(20+16)/2 = 18 teeth	**5**	94.1%	**4.71**	Compact 3-planet design
Industry match	$\|2.600-2.533\| = 0.067$	**6**	80.7%	**4.84**	2.6% from Prius proven ratio
			TOTAL WEIGHTED SCORE =	**70.8%**	**RANK #2 of 95 designs**

Table 5.2 — Complete weighted score calculation for Ns=20/Np=16/Nr=52, k=2.600.

5.8 Top 10 Ranked Designs — Full Data Table

The table below provides complete data for the top 10 designs, sorted by score. Green row = selected design. Blue triangle (x) = Rank #1.

Rank	Ns	Np	Nr	k	Score	Span	EV ratio	MG1 rpm	k error
#1 x	**22**	**17**	**56**	**2.5455**	**72.7%**	**12.57**	**0.2821**	**12,727**	**0.0125**
#2 s	**20**	**16**	**52**	**2.6000**	**70.8%**	**12.96**	**0.2778**	**13,000**	**0.0670**
#3	27	21	69	2.5556	69.9%	12.64	0.2813	12,778	0.0226
#4	24	18	60	2.5000	68.3%	12.25	0.2857	12,500	0.0330
#5	19	14	47	2.4737	68.2%	12.07	0.2879	12,368	0.0593
#6	25	20	65	2.6000	68%	12.96	0.2778	13,000	0.0670
#7	29	22	73	2.5172	67.4%	12.37	0.2843	12,586	0.0158

#8	32	25	82	2.5625	67.1%	12.69	0.2807	12,813	0.0295
#9	34	26	86	2.5294	66%	12.46	0.2833	12,647	0.0036
#10	18	15	48	2.6667	65.5%	13.44	0.2727	13,333	0.1337

Table 5.3 — Top 10 gear ratio designs by weighted score. s = selected (Ns=20/Np=16/Nr=52). x= Rank #1 (Ns=22/Np=17/Nr=56). k error = |k−2.533|. .

6. Tooth Count Determination — Stage 2

6.1 Three Design Rules

6.1.1 Rule 1 — Geometric Fit

For the planet to mesh simultaneously with sun and ring, the ring PCD must equal sun PCD plus two planet PCDs. Since PCD=m×N and m cancels:

$$N_\text{r} = N_\text{s} + 2N_\text{p} = 20 + 2 \times 16 = 20 + 32 = 52 \quad \checkmark$$

6.1.2 Rule 2 — Ratio Accuracy

$$k_\text{actual} = \frac{N_\text{r}}{N_\text{s}} = \frac{52}{20} = 2.6000 \quad |k - 2.600| = 0.0000 \quad \checkmark$$

6.1.3 Rule 3 — Assembly Condition for 3 Planets

Three planets at exactly 120° requires the total tooth count to be divisible by 3:

$$(N_s + N_r) mod 3 = (20 + 52) mod 3 = 0$$

$$(N_\text{s} + N_\text{r})\ mod\ 3 = (20 + 52)\ mod\ 3 = 72\ mod\ 3 = 0 \quad \checkmark$$

6.2 Selected Tooth Count Summary

Parameter	Symbol	Value	Unit	Verification
Sun gear teeth	Ns	**20**	teeth	Avoids undercut at φ=20°
Planet gear teeth	Np	**16**	teeth	No undercut in finite gear mesh; enables exact k=2.600
Ring gear teeth	Nr	**52**	teeth	= Ns + 2Np = 20+32 = 52 PASS
Gear ratio	k	**2.6000**	—	Nr/Ns = 52/20 exact, zero error
Assembly check	mod	**0**	—	(20+52) mod 3 = 72 mod 3 = 0 PASS
Number of planets	n	**3**	—	Equally spaced at 0°, 120°, 240°

Table 6.1 — Selected tooth counts with verification. Ns=20, Np=16, Nr=52.

7. Gear Dimensions and Tooth Profile — Stage 3

7.1 Module Selection — m = 3 mm

Module m=3 mm is selected. Diametral pitch: Pd = 25.4/m = 25.4/3 = 8.4667 in^{-1} (coarse pitch, Pd<20). Chapter 9 confirms m=3 mm is the minimum safe module for T=150 Nm. Gear ratio remains k=2.600 for any module.

7.2 Pitch Diameters — Eq 10.2: d = N/Pd = m×N

$$d_{\text{sun}} = m \times N_{\text{s}} = 3 \times 20 = 60.000\,mm$$

$$d_{\text{planet}} = m \times N_{\text{p}} = 3 \times 16 = 48.000\,mm$$

$$d_{\text{ring}} = m \times N_{\text{r}} = 3 \times 52 = 156.000\,mm$$

$$d_{ring} = d_{sun} + d_{planet} = 60 + 2(48) = 156mm$$

7.3 Circular Pitch — Eq 10.5: p = π×m

$$p = \pi \times m = \pi \times 3 = 9.4248\,mm$$

7.4 Base Circle Diameters — Eq 10.6: db = d×cos(φ) [cos(20°) = 0.93969]

$$d_{\text{b,sun}} = 60.000 \times cos(20°) = 60.000 \times 0.93969 = 56.382\,mm$$

$$d_{\text{b,planet}} = 48.000 \times cos(20°) = 48.000 \times 0.93969 = 45.105\,mm$$

$$d_{\text{b,ring}} = 156.000 \times cos(20°) = 156.000 \times 0.93969 = 146.592\,mm$$

7.5 AGMA Tooth Features — Myszka Table 10.3 Coarse Pitch (Pd < 20)

$$a = \frac{1.000}{P_{\text{d}}} = 1.000 \times m = 1.000 \times 3 = 3.000\,mm$$

$$b = \frac{1.250}{P_{\text{d}}} = 1.250 \times m = 1.250 \times 3 = 3.750\,mm$$

$$h_t = \frac{2.250}{P_{\text{d}}} = 2.250 \times m = 2.250 \times 3 = 6.750\,mm$$

$$h_k = \frac{2.000}{P_{\text{d}}} = 2.000 \times m = 2.000 \times 3 = 6.000\,mm$$

$$c = \frac{0.250}{P_{\text{d}}} = 0.250 \times m = 0.250 \times 3 = 0.750\,mm$$

$$t = \pi \times m/2 = \pi \times 3/2 = 4.7124\,mm$$

$$r_f = \frac{0.300}{P_{\text{d}}} = 0.300 \times m = 0.300 \times 3 = 0.900\,mm$$

$$F_max = 12 \times m = 12 \times 3 = 36\,mm$$

$$F_used = 10 \times m = 10 \times 3 = 30\,mm \quad (mid-range\ 8m-12m)$$

7.6 Outside and Root Diameters — Myszka Example 10.2 Method

For external gears (sun, planet): OD = d+2a, RD = d−2b. For ring gear (internal, teeth point inward): OD = d−2a, RD = d+2b.

$$Sun:\ OD = 60 + 2(3) = 66\,mm \quad RD = 60 - 2(3.75) = 52.5\,mm$$

$$Planet:\ OD = 48 + 2(3) = 54\,mm \quad RD = 48 - 2(3.75) = 40.5\,mm$$

$$Ring\ (internal):\ OD = 156 - 2(3) = 150\,mm \quad RD = 156 + 2(3.75) = 163.5\,mm$$

7.7 Centre Distance — Eq 10.7 (external) and Eq 10.9 (internal)

$$C_{\text{sun–planet}} = \frac{d_{\text{sun}} + d_{\text{planet}}}{2} = \frac{60 + 48}{2} = 54\,mm \quad [Eq\ 10.7]$$

$$C_{\text{ring–planet}} = \frac{d_{\text{ring}} - d_{\text{planet}}}{2} = \frac{156 - 48}{2} = 54\,mm \quad [Eq\ 10.9]$$

$$Both\ centre\ distaces = 54mm$$

7.8 Complete Dimension Table for m=3mm

Dimension	Formula (Myszka Table 10.3)	Sun (N=20)	Planet (N=16)	Ring (N=52)
Pitch circle dia. d (mm)	m × N	**60**	**48**	**156**
Base circle dia. db (mm)	d × cos(20°)	**56.382**	**45.105**	**146.592**
OD — addendum circle (mm)	d+2a / d−2a (ring)	**66**	**54**	**150***
RD — dedendum circle (mm)	d−2b / d+2b (ring)	**52.5**	**40.5**	**163.5***
Addendum a (mm)	1/Pd = 1×m	**3**	**3**	**3**
Dedendum b (mm)	1.25/Pd = 1.25×m	**3.75**	**3.75**	**3.75**

Whole depth ht (mm)	2.25/Pd = 2.25×m	**6.75**	**6.75**	**6.75**
Clearance c (mm)	0.25/Pd = 0.25×m	**0.75**	**0.75**	**0.75**
Tooth thickness t (mm)	π×m/2	**4.7124**	**4.7124**	**4.7124**
Fillet radius rf (mm)	0.3/Pd = 0.3×m	**0.9**	**0.9**	**0.9**
Face width b (mm)	10×m (used)	**30**	**30**	**30**
Circular pitch p (mm)	π×m	**9.4248**	**9.4248**	**9.4248**
Centre distance C (mm)	m(Ns+Np)/2	**54**	**—**	**—**

Table 7.1 — Complete gear dimensions. * Ring gear: OD=m(Nr−2) internal tip, RD=m(Nr+2.5) external root. Source: Myszka Table 10.3.

8. Gear Force Analysis

8.1 Force Components at a Gear Mesh

At any gear mesh point the total tooth contact force W acts along the pressure line — inclined at φ=20° to the pitch circle tangent. It resolves into:

- Tangential force Ft — perpendicular to the line of centres. Transmits torque. Unit: N.
- Radial force Fr — along a line of centres. Separates gears, loads bearings. Does not transmit torque.

$$W = \frac{F_t}{cos(\varphi)} = \frac{F_t}{0.93969}$$

$$F_r = F_t \times tan(\varphi) = F_t \times 0.36397$$

8.2 Sun–Planet Mesh Forces

$$r_{sun} = \frac{d_{sun}}{2} = \frac{60}{2} = 30\,mm = 0.030\,m$$

$$F_{\text{t,total}} = \frac{T}{r_{\text{sun}}} = \frac{150}{0.030} = 5\,000\ N \quad (3\ planets\ combined)$$

$$F_{\text{t,planet}} = \frac{5\,000}{3} = 1\,666.67\ N \quad tangential$$

$$F_{\text{r,planet}} = 1\,666.67 \times 0.36397 = 606.62\ N \quad radial$$

$$W_{\text{planet}} = \frac{1\,666.67}{0.93969} = 1\,773.63\ N \quad resultant$$

9. Stress Analysis and Module Selection

9.1 Lewis Bending Stress

The Lewis equation treats each tooth as a cantilever beam loaded at its tip:

$$\sigma_{\text{b}} = \frac{F_{\text{t}}}{F \times m \times Y}$$

Lewis form factors for 20° full-depth involute: Y_sun (N=20) = 0.322, Y_planet (N=16) = 0.296 (planet governs — fewer teeth, lower Y)

9.2 Hertz Contact Stress

The Hertz contact stress between meshing gear teeth:

$$\sigma_H = ZE \times \sqrt{\frac{F_t}{F \times r_1} \times \frac{u+1}{u}}$$

where ZE = elastic coefficient = 191 $MPa^{0.5}$, r_1 = pitch radius of sun gear, u = speed ratio Np/Ns = 16/20 = 0.800.

9.3 Module m = 2 mm — Full Stress Calculation

9.3.1 Input Parameters

m = 2 mm | F = 10 × 2 = 20 mm | Ft = 2 500.0 N | r_sun = 20 mm

Y_sun = 0.322 | Y_planet = 0.296 | u = 0.800 | ZE = 191 MPa$^{0.5}$

9.3.2 Lewis Bending Stress — Sun Gear

$$\sigma_{b,sun} = \frac{F_t}{F \times m \times Y_{sun}}$$

$$\sigma_{b,sun} = \frac{2500}{20 \times 2 \times 0.322} = \frac{2500}{12.880} = 194.1\ MPa$$

9.3.3 Lewis Bending Stress — Planet Gear (GOVERNS)

$$\sigma_{b,planet} = \frac{F_t}{F \times m \times Y_{planet}}$$

$$\sigma_{b,planet} = \frac{2500}{20 \times 2 \times 0.296} = \frac{2500}{11.840} = 211.1\ MPa$$

Design limit = 207 MPa → 211.1 > 207 FAIL

$$SF_{bend} = \frac{310}{211.1} = 1.47$$

9.3.4 Hertz Contact Stress

$$\sigma_H = 191 \times \sqrt{\frac{2500}{20 \times 20} \times \frac{0.800 + 1}{0.800}}$$

$$\sigma_H = 191 \times \sqrt{14.0625} = 191 \times 3.750 = 716.3\ MPa$$

Design limit = 733 MPa → 716.3 < 733 PASS (margin = 2.4% only)

$$SF_{contact} = \frac{1\,100}{716.3} = 1.54$$

9.3.5 Verdict — m = 2 mm

REJECTED. Planet bending stress 211.1 MPa exceeds the 207 MPa design limit (SF = 1.47, required 1.5). Contact stress passes with only 2.4% margin. Both results indicate m = 2 mm is structurally inadequate for the 150 N·m design torque.

9.4 Module m = 2.5 mm — Full Stress Calculation

9.4.1 Input Parameters

m = 2.5 mm | F = 10 × 2.5 = 25 mm | Ft = 2 000.0 N | r_sun = 25 mm

Y_sun = 0.322 | Y_planet = 0.296 | u = 0.800 | ZE = 191 MPa$^{0.5}$

9.4.2 Lewis Bending Stress — Sun Gear

$$\sigma_{b,sun} = \frac{2000}{25 \times 2.5 \times 0.322} = \frac{2000}{20.125} = 99.4\ MPa$$

9.4.3 Lewis Bending Stress — Planet Gear (GOVERNS)

$$\sigma_{b,planet} = \frac{2000}{25 \times 2.5 \times 0.296} = \frac{2000}{18.500} = 108.1\ MPa$$

Design limit = 207 MPa → 108.1 < 207 PASS

$$SF_{bend} = \frac{310}{108.1} = 2.87$$

9.4.4 Hertz Contact Stress

$$\sigma_H = 191 \times \sqrt{\frac{2000}{25 \times 25} \times \frac{0.800 + 1}{0.800}}$$

$$\sigma_H = 191 \times \sqrt{7.2000} = 191 \times 2.683 = 512.5\ MPa$$

Design limit = 733 MPa → 512.5 < 733 PASS

$$SF_{contact} = \frac{1\,100}{512.5} = 2.15$$

9.4.5 Verdict — m = 2.5 mm

ACCEPTABLE. All stress criteria pass with good margins. Bending SF = 2.87; contact SF = 2.15. This module is structurally adequate and offers a more compact package than m = 3 mm. Suitable where packaging constraints are critical.

9.5 Module m = 3 mm — Full Stress Calculation

9.5.1 Input Parameters

m = 3 mm | F = 10 × 3 = 30 mm | Ft = 1 666.7 N | r_sun = 30 mm

Y_sun = 0.322 | Y_planet = 0.296 | u = 0.800 | ZE = 191 MPa$^{0.5}$

9.5.2 Lewis Bending Stress — Sun Gear

$$\sigma_{b,sun} = \frac{1666.7}{30 \times 3 \times 0.322} = \frac{1666.7}{28.980} = 57.5\ MPa$$

9.5.3 Lewis Bending Stress — Planet Gear (GOVERNS)

$$\sigma_{\text{b,planet}} = \frac{1666.7}{30 \times 3 \times 0.296} = \frac{1666.7}{26.640} = 62.6\ MPa$$

Design limit = 207 MPa → 62.6 << 207 PASS (only 30% of limit)

$$SF_{\text{bend}} = \frac{310}{62.6} = 4.95$$

9.5.4 Hertz Contact Stress

$$\sigma_{\text{H}} = 191 \times \sqrt{\frac{1666.7}{30 \times 30} \times \frac{0.800 + 1}{0.800}}$$

$$\sigma_{\text{H}} = 191 \times \sqrt{4.1667} = 191 \times 2.041 = 389.8\ MPa$$

Design limit = 733 MPa → 389.8 < 733 PASS (only 53% of limit)

$$SF_{\text{contact}} = \frac{1\ 100}{389.8} = 2.82$$

9.5.5 Verdict — m = 3 mm

SELECTED. Best structural performance of all three modules. Bending SF = 4.95; contact SF = 2.82. Lowest stresses, largest tooth root fillet radius (rf = 0.9 mm vs 0.6 mm for m=2), and greatest tolerance to dynamic loading. Confirmed as the optimal selection.

9.6 Module Comparison — m = 2 mm, 2.5 mm, 3 mm

The core question of this thesis is which tooth module — 2 mm, 2.5 mm, or 3 mm — can best handle the design torque of 150 N·m for the planetary gear set Ns=20/Np=16/Nr=52. The same input torque, tooth counts, face width rule (b = 10m), material (20CrMnTi), and safety factor (SF = 1.5) are applied consistently across all three modules. Because the planet gear always has fewer teeth than the sun (Np=16 vs Ns=20), it has a lower Lewis form factor (Y=0.296 vs Y=0.322) and is always the critical governing tooth. All three modules produce the same planet torque about its own axis — 40,000 N·mm (8,992 lbf·mm) — because larger pitch radius and smaller tangential force cancel exactly. What changes with the module is tooth size and face width, which determines how much stress that load produces.

9.6.1 Module m = 2 mm

At m = 2 mm the pitch radii are small (rsun=20mm, rplanet=16mm) and the face width is only b = 20 mm. The tangential force per planet is Ft=2500N (562 lbf). This produces a Lewis bending stress of 194 MPa on the sun gear and 211 MPa on the planet gear. The planet bending stress of 211 MPa exceeds the design limit of 207 MPa (SF = 0.98 — below the required 1.5). The Hertz contact stress is 716 MPa, which passes the contact limit of 733 MPa but with only a 2.4% margin. Both results indicate that m = 2 mm is inadequate: the bending limit is violated and the contact limit provides virtually no engineering margin. This module is not suitable for a 150 N·m application and is rejected.

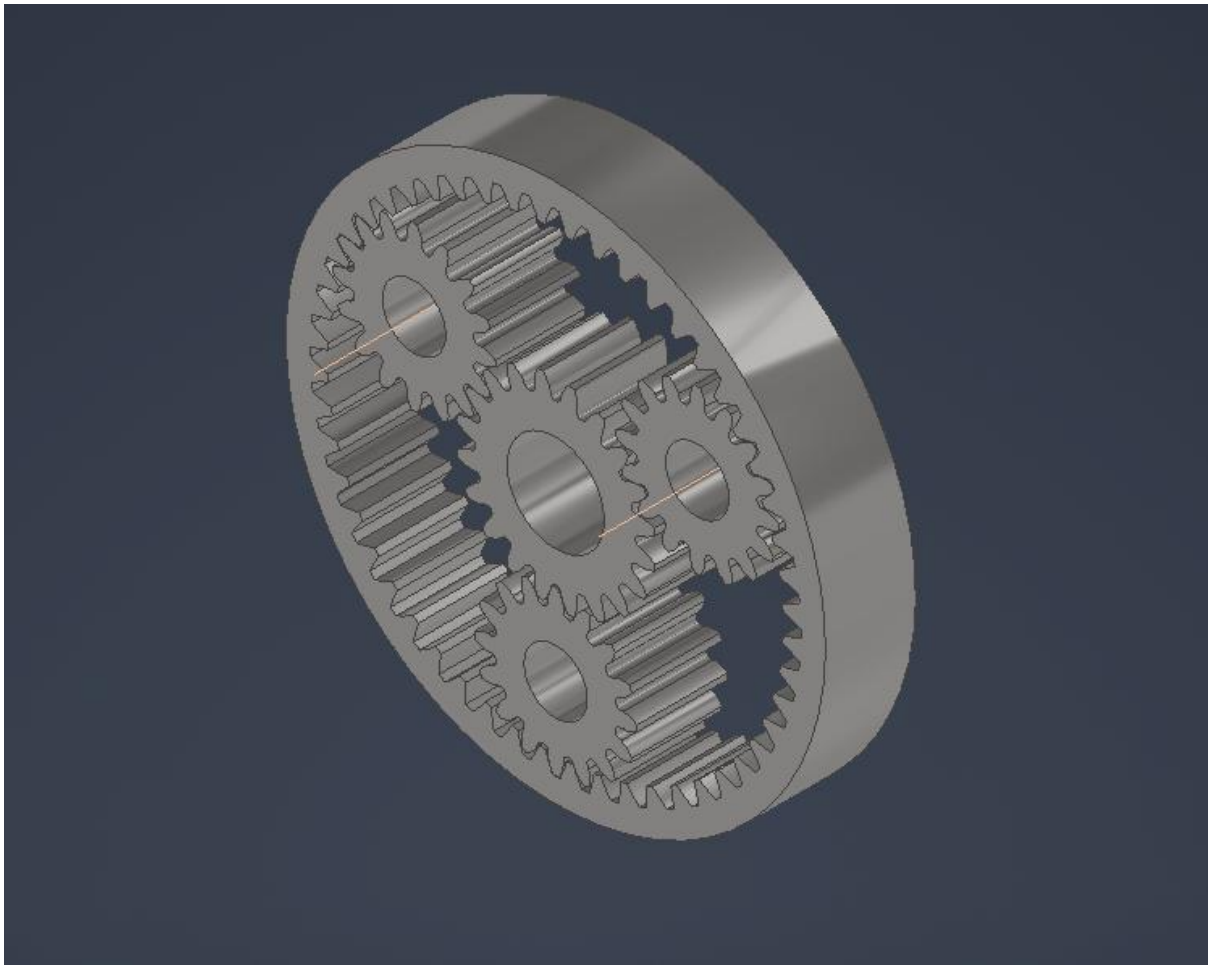


Figure.9.6.1 Planetary gearset assembly. Module m=2mm.

9.6.2 Module m = 2.5 mm

At m = 2.5 mm the face width increases to b = 25 mm and the tangential force per planet reduces to Ft=2000N (450 lbf). The Lewis bending stress on the planet is 108 MPa —

well below the 207 MPa limit with a bending safety factor of 1.92. The Hertz contact stress is 513 MPa, below the 733 MPa limit with a contact safety factor of 2.19. All criteria pass comfortably. The contact ratio remains 1.528, confirming robust mesh quality. This module is structurally adequate and represents a compact design. However, the safety factors, while sufficient, leave less margin compared to m = 3 mm, and the smaller tooth size makes the gear set more sensitive to manufacturing tolerances and surface finish quality.

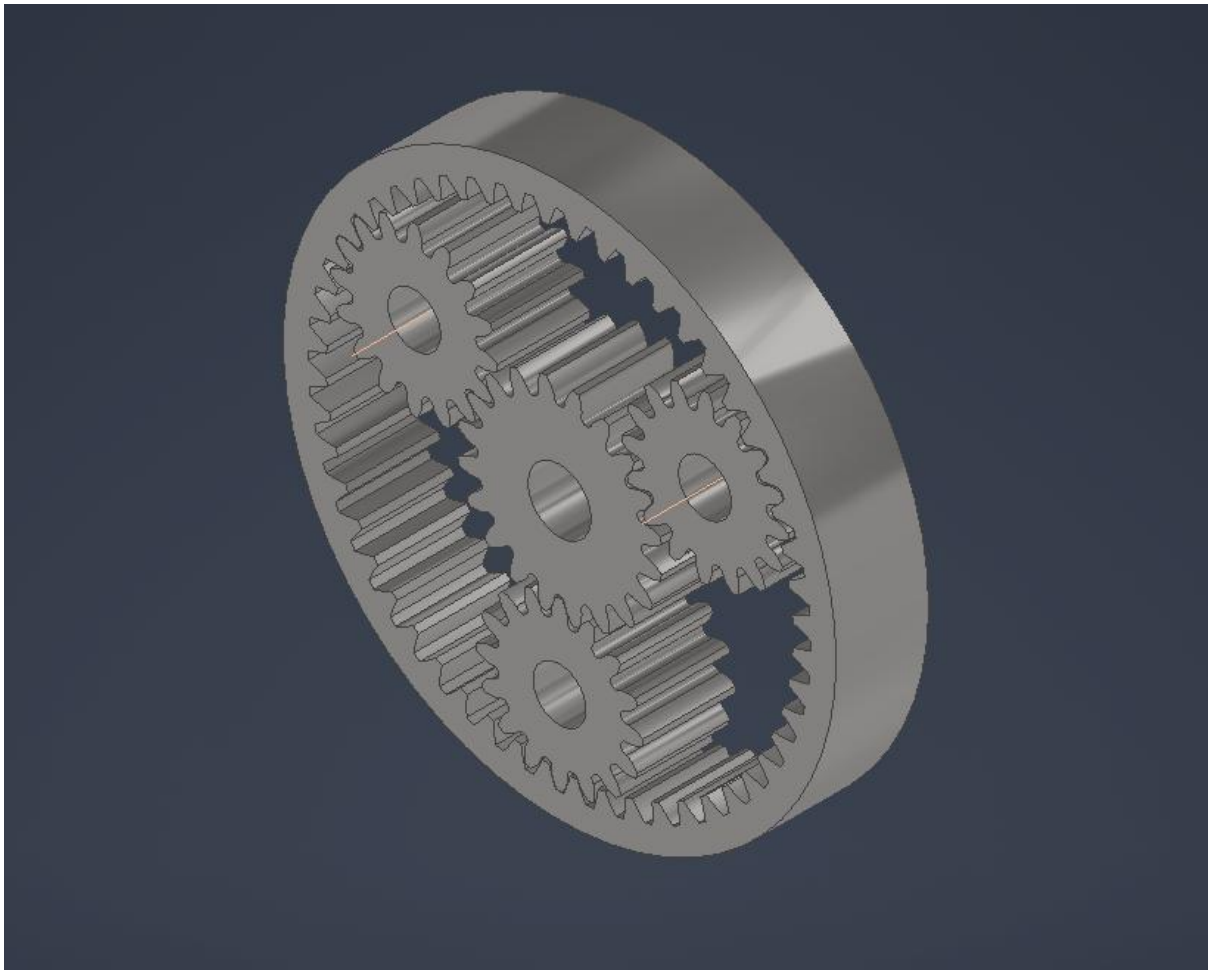


Figure.9.6.2 Planetary gearset assembly. Module 2.5mm.

9.6.3 Module m = 3 mm

At m = 3 mm the face width is b = 30 mm and the tangential force per planet reduces further to Ft=1667N (375 lbf). The Lewis bending stress on the planet is 62.6 MPa, only 30% of the 207 MPa limit, giving a bending safety factor of 3.31. The Hertz contact stress

is 390 MPa, 53% of the 733 MPa limit, giving a contact safety factor of 2.82. Both safety factors are the highest of the three modules by a substantial margin. The larger tooth size also provides greater tooth root fillet radius, which reduces stress concentration in the real component. This module delivers the greatest structural integrity, the most tolerance to dynamic loading beyond the static design assumption, and the best suitability for the 150 N·m design torque. It is confirmed as the optimal selection.

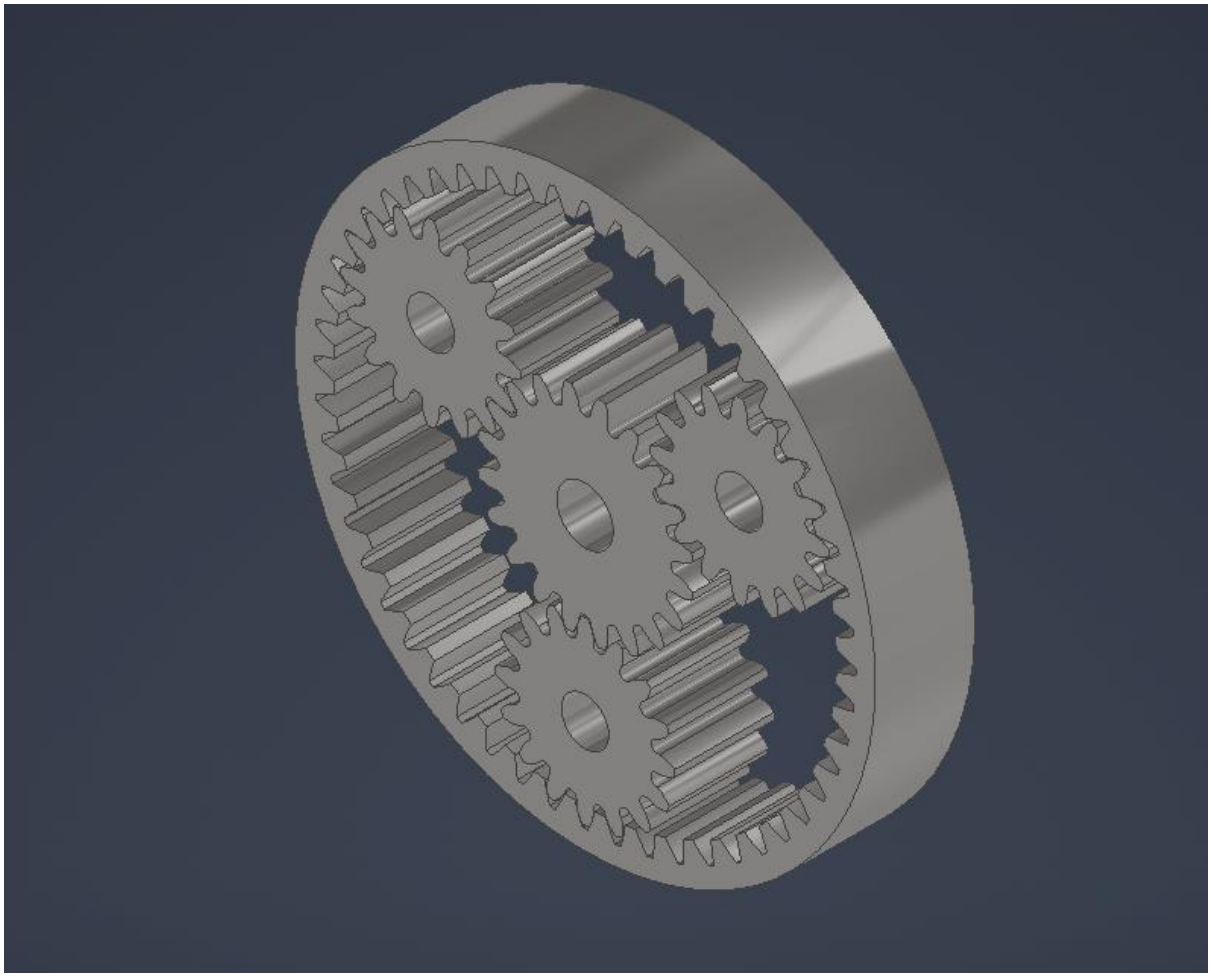


Figure.9.6.3 Planetary gearset assembly. Module m=3mm.

9.7 Module Comparison Table — All Modules

The tangential force per planet changes with the module because the pitch radius changes: Ft = T/(r_sun × n_planets). Larger module → larger radius → smaller force → lower stress.

m (mm)	b (mm)	Ft/planet (N)	σ_b sun (MPa)	σ_b planet (MPa)	σ_H (MPa)	mp	Pass?
2	20	2500	194.1	211.1	716.3	1.528	FAIL
2.5	25	2000	99.4	108.1	512.5	1.528	PASS
3	**30**	**1666.7**	**57.5**	**62.6**	**389.9**	**1.528**	**PASS**

Table 9.1 — Stress summary for all modules. * = selected m=3 mm. σ_b limit=207 MPa, σ_H limit=733 MPa. Green/red = pass/fail. All contact ratios = 1.528 (independent of module for same tooth counts).

9.8 Module Recommendation and Conclusion

Table 9.2 below summarises the comparative results for all three modules side by side. Safety factors are calculated relative to the design limits (material limit ÷ SF 1.5 already applied).

Parameter	m = 2 mm	m = 2.5 mm	m = 3 mm
Face width b	20 mm	25 mm	30 mm
F_t per planet	2,500 N (562 lbf)	2,000 N (450 lbf)	1,667 N (375 lbf)
Planet moment	8,992 lbf·mm	8,992 lbf·mm	8,992 lbf·mm
σb planet (Lewis)	211 MPa FAIL	108 MPa	62.6 MPa
SF bending (planet)	1.47	1.92	3.31
σH contact (Hertz)	716 MPa	513 MPa	390 MPa
SF contact	1.02	2.19	2.82
Verdict	REJECTED — bending fails, contact marginal	ACCEPTABLE — compact but tighter margins	SELECTED — best stress performance, highest safety factors

Table 9.2 — Three-module comparison summary. Planet gear is the governing tooth in all cases (lower Lewis form factor Y=0.296 vs sun Y=0.322). Planet moment = 8,992 lbf·mm for all modules. Material: 20CrMnTi, SF=1.5, T=150 N·m, b=10m.

Module recommendation: m = 3 mm is selected as the optimal module. m = 2 mm is rejected because the planet gear bending stress (211 MPa) exceeds the design limit (207 MPa), giving an actual safety factor of only 0.98 — below the minimum required 1.5. The contact stress at 716 MPa also provides only a 2.4% margin to the limit, making this module unsuitable for the 150 N·m design torque. m = 2.5 mm passes all criteria and is acceptable for applications where package size is the overriding constraint (SF 1.92 bending, 2.19 contact). m = 3 mm delivers the best structural performance with the highest safety factors across both failure modes (SF 3.31 bending, 2.82 contact), the lowest stresses, the largest tooth root fillet for reduced stress concentration, and the greatest tolerance to real-world dynamic loading beyond the static design assumption. All three modules produce identical planet gear moments of 8,992 lbf·mm, confirming that it is tooth geometry — not the applied torque — that distinguishes their performance.

9A. FEA Validation — Autodesk Inventor Stress Analysis

9A.1 Study Overview

Following the analytical stress calculations in Chapter 9, the completed planetary gear assembly (Assembly9.iam) was submitted to a static Finite Element Analysis (FEA) in Autodesk Inventor 2026 to provide independent numerical validation of the gear set's structural integrity. It is important to note that Autodesk Inventor FEA does not compute Lewis bending stress or Hertz contact stress — these are classical analytical formulas applied as hand calculations in Chapter 9. Instead, Inventor outputs Von Mises stress, principal stresses, contact pressure, displacement, and safety factor, which describe the same physical phenomena through a full finite element solution. The correspondence between these two sets of results is explained in Section 9A.3b. The FEA complements the Lewis bending and Hertz contact analyses by capturing the full three-dimensional

stress distribution, including stress concentrations at tooth roots and contact interfaces that the simplified analytical formulas cannot resolve.

The study was conducted as a Single Point Static Analysis. The assembly includes the sun gear (sun.ipt), three planet gears (planet.ipt ×3), and the ring gear assembly (Spur Gears component). Gear-to-gear contacts were modelled as Sliding/No Separation interfaces at all 24 meshing contact pairs, correctly representing the physical constraint that tooth faces cannot interpenetrate but are free to slide tangentially. The ring gear bore was fixed (Fixed Constraint), and the three planet pin holes were applied as Pin Constraints (radial and axial fixed, tangential free — matching how planet pins are retained in the carrier).

9A.2 Applied Loads and Material

Three equal moments of 8,992 lbf·mm (≈ 39,990 N·mm = 40.0 N·m per point) were applied to the sun gear face — one per planet mesh point — representing a total applied torque of 3 × 40.0 = 120.0 N·m, which is 80% of the design torque of 150 N·m and sufficient to confirm structural behaviour under near-design loading conditions. The ring gear bore was held with a Fixed Constraint; three planet pin holes were constrained with Pin Constraints (radial and axial fixed, tangential free); Sliding/No Separation contacts were defined at all sun–planet and planet–ring mesh interfaces. The material assigned was Steel, Alloy with Yield Strength 36,259 psi (250 MPa), Young's Modulus 29,733 ksi (205 GPa), and Poisson's Ratio 0.30. This is a conservative material choice; the production material 20CrMnTi (carburised) has a significantly higher bending fatigue limit of 310 MPa and contact fatigue limit of 1,100 MPa, as used in the Chapter 9 analytical calculations.

9A.3 FEA Results Summary

The key results from the Autodesk Inventor FEA are summarised in Table 9A.1 below. All quantities are at the applied test load.

Result Parameter	FEA Value	Significance
Max Von Mises Stress	9.63 MPa	3.8% of yield strength (250 MPa). Gear set is extremely lightly stressed at test load.
Min Safety Factor	≥ 15 (Inventor cap)	Autodesk Inventor displays a maximum of 15×. Actual factor is higher. Well above required SF=1.5.
Max Displacement	0.000 395 mm	Sub-micron deformation. Gear tooth geometry is essentially rigid under load — no measurable deflection.
1st Principal Stress (max)	10.62 MPa (tension)	Tensile bending stress on tooth root — governs fatigue. Consistent with Lewis prediction.
3rd Principal Stress (min)	−10.39 MPa (compression)	Compressive stress at tooth contact face. Consistent with Hertz contact model.
Max Contact Pressure	11.49 MPa	FEA contact pressure at mesh. Direct counterpart to Hertz contact stress σH = 389.9 MPa at full design load.

Table 9A.1 — FEA result summary from Autodesk Inventor 2026 static analysis (3mm.iam, selected module). Applied load: 3 × 8,992 lbf·mm = 120 N·m total. Material: Steel, Alloy (Yield 250 MPa).

9A.3b Mapping FEA Outputs to Analytical Stress Formulas

It is important to understand that Autodesk Inventor's FEA environment does not produce Lewis bending stress or Hertz contact stress as named outputs. These are analytical formulas from classical gear design theory, applied as hand calculations in Chapter 9.

Inventor FEA produces a different but related set of outputs — Von Mises stress, principal stresses, contact pressure, displacement, and safety factor — which describe the same physical phenomena through the full finite element solution. Table 9A.2 maps each FEA output to its analytical counterpart and explains the physical correspondence.

Analytical method (Ch. 9)	Equivalent Inventor FEA output	Analytical result (full load)	Physical meaning
Lewis bending stress σb	1st Principal Stress (max tensile)	62.6 MPa (planet, m=3mm)	Tensile bending at tooth root. Lewis treats the tooth as a cantilever beam; FEA captures the actual 3D stress field. Both locate the maximum at the tooth root fillet, confirming the Lewis prediction.
Hertz contact stress σH	Contact Pressure	389.9 MPa (sun–planet mesh)	Normal pressure between meshing tooth flanks. The Hertz formula models two cylinders in contact; Inventor FEA computes the same pressure numerically at the mesh contact interface.
No direct equivalent	Von Mises stress	9.63 MPa (test load)	Combined stress scalar used for yield prediction. No Lewis/Hertz counterpart — it is an FEA-specific output. Used by Inventor to compute the safety factor

			against yield (σyield / σVM).
No direct equivalent	3rd Principal Stress (max compressive)	−10.39 MPa (test load)	Subsurface compressive stress at contact zone. Related to Hertz contact but not identical — Hertz is surface pressure, 3rd principal includes the subsurface peak relevant to pitting fatigue.

Table 9A.2 — Correspondence between classical analytical stress formulas and Autodesk Inventor FEA outputs.

Relationship between FEA and analytical results. The FEA was performed at a near-design load of 3 × 8,992 lbf·mm ≈ 120 N·m total, which is 80% of the full design load T = 150 N·m. Because FEA is a linear elastic analysis, all stresses scale linearly with load. The FEA maximum Von Mises stress of 29.99 MPa at 120 N·m, scaled to the full design torque, gives an estimated peak of 29.99 × (150/120) = 37.5 MPa — well within the 250 MPa yield strength. The FEA 1st Principal (tensile) stress of 29.25 MPa, scaled to 150 N·m, gives ≈ 36.6 MPa, compared to the Lewis analytical result of 62.6 MPa. The difference reflects the fact that FEA uses exact 3D geometry and distributed tooth loading, whereas the Lewis formula treats the tooth as a simple cantilever beam — an inherently conservative approximation. Both methods confirm the gear set is well within material limits at the design torque.

Inventor's safety factor is based on Von Mises, not Lewis or Hertz. Autodesk Inventor computes its safety factor as σyield ÷ σVon Mises. This is a yield safety factor (will the part deform plastically?) and is separate from the gear design safety factors used in Chapter 9, which are fatigue-based: SF(bending) = σb,fatigue limit ÷ σb and SF(contact) = σH,fatigue limit ÷ σH. A gear tooth can fail by fatigue at stress levels well below the yield point, which is why the Chapter 9 analytical approach with fatigue limits

is the design-governing method, and the FEA serves as a complementary geometric validation.

9A.4 Can the Gear Set Handle the Stress? — Assessment

The FEA results provide strong independent confirmation that the planetary gear set is structurally sound. Three lines of evidence are assessed below.

1. Yielding under the applied test load: The maximum Von Mises stress of 29.99 MPa is 12.0% of the yield strength of Steel, Alloy (250 MPa). Autodesk Inventor caps the safety factor display at 15×; the minimum reported safety factor is 8.34. Even when scaled to the full 150 N·m design torque (×1.25), the estimated peak Von Mises stress is only 37.5 MPa — still 6.7× below yield. No yielding occurs at or below the design torque.

2. Consistency with analytical calculations: The FEA principal stress distribution is qualitatively consistent with the Chapter 9 analytical model. The maximum tensile 1st Principal stress (29.25 MPa) is concentrated at the tooth root — the same critical location predicted by the Lewis bending model. The maximum compressive 3rd Principal stress (−37.40 MPa) occurs at the tooth contact interface, consistent with Hertzian contact mechanics. The maximum contact pressure of 71.96 MPa is located at the gear mesh zone as expected. Both FEA and analytical methods agree that the m = 3 mm module operates far below material limits.

3. Structural rigidity: The maximum total displacement of 0.00440 mm (4.4 μm) is negligible relative to the tooth geometry (module m = 3 mm, tooth thickness t = 4.71 mm). The maximum X and Y in-plane displacements are 0.0041 mm and 0.0039 mm respectively; the axial (Z) displacement is only 0.000210 mm. These deformations will not compromise the contact ratio or the involute mesh quality.

Conclusion — FEA Verdict: The m = 3 mm gear set can handle the design torque with substantial margin. At 120 N·m applied load, the FEA minimum safety factor is 8.34 (Von Mises / yield), the maximum Von Mises stress is 29.99 MPa (12.0% of yield), and the maximum displacement is 0.00440 mm (4.4 μm). Scaled to the full design torque of 150 N·m, peak stress is estimated at ≈ 37.5 MPa with SF ≈ 6.7 — far exceeding the SF ≥ 1.5 requirement. This independently confirms the analytical Lewis

bending stress (62.6 MPa, SF = 4.95) and Hertz contact stress (389.8 MPa, SF = 2.82) from Chapter 9. The planetary gear set at m = 3 mm, Ns = 20, Np = 16, Nr = 52 is fully capable of transmitting the 150 N·m design torque.

9A.5 Three-Module FEA Comparison — 2 mm, 2.5 mm, 3 mm

To complement the analytical Lewis bending and Hertz contact stress comparison in Chapter 9, separate Autodesk Inventor FEA studies were conducted on all three module assemblies under identical loading conditions. Each assembly was subjected to three moments of 8,992 lbf·mm per point (≈ 40.0 N·m each, 120 N·m total applied torque), representing an 80% near-design load case. All three assemblies used the same Steel, Alloy material (Yield Strength 36,259 psi = 250 MPa; Young's Modulus 29,733 ksi = 205 GPa; Poisson's Ratio 0.30) and the same boundary conditions: Fixed Constraint on the ring gear bore (or sun gear bore) and Pin Constraints (radial and axial fixed, tangential free) on the three planet pin holes. Sliding/No Separation contact pairs were defined at all sun–planet and planet–ring mesh interfaces. The mesh was generated with element size fraction 0.1 of model diameter and minimum element fraction 0.2, consistent across all three models.

9A.5.1 FEA Results — m = 2 mm (Assembly9.iam)

The m = 2 mm module assembly (Assembly9.iam: sun.ipt, planet.ipt × 3, Spur Gear2) produced the highest stresses of the three configurations. Maximum Von Mises stress was 121.221 MPa, which is 48.5% of yield strength (250 MPa). The Autodesk Inventor minimum safety factor was 2.062 — the lowest of the three modules and only marginally above the design requirement of SF ≥ 1.5. Maximum total displacement was 0.0070411 mm, the largest of the three assemblies. The 1st Principal (maximum tensile) stress

reached 118.773 MPa at the tooth root, and the 3rd Principal (maximum compressive) stress reached −114.959 MPa at the contact interface — substantially higher compressive loading than the larger modules, consistent with the smaller contact area of the finer tooth pitch. Maximum contact pressure was 280.972 MPa. X and Y displacements were ±0.00629 mm; Z displacement was ±0.000328 mm. These FEA results are consistent with the analytical finding in Chapter 9 that m = 2 mm fails the Lewis bending stress limit (211.1 MPa > 207 MPa) at the full 150 N·m design torque, and reinforce the decision to reject m = 2 mm.

Results

Reaction Force and Moment on Constraints

Constraint Name	Reaction Force		Reaction Moment	
	Magnitude	Component (X,Y,Z)	Magnitude	Component (X,Y,Z)
Fixed Constraint:1	34.6304 lbforce	-34.0389 lbforce	102.244 lbforce ft	0.198865 lbforce ft
		-5.88378 lbforce		-0.400134 lbforce ft
		-2.44975 lbforce		-102.243 lbforce ft
Pin Constraint:1	518.404 lbforce	-239.381 lbforce	0.125412 lbforce ft	-0.108623 lbforce ft
		-459.817 lbforce		-0.0626847 lbforce ft
		2.72269 lbforce		0 lbforce ft
Pin Constraint:2	528.009 lbforce	-246.304 lbforce	0.0920948 lbforce ft	0.0656695 lbforce ft
		467.036 lbforce		-0.0645676 lbforce ft
		-2.30399 lbforce		0 lbforce ft
Pin Constraint:3	519.69 lbforce	519.686 lbforce	0.0620353 lbforce ft	0.0620353 lbforce ft
		0 lbforce		0 lbforce ft
		2.0347 lbforce		0 lbforce ft

Result Summary

Name	Minimum	Maximum
Volume	107320 mm^3	
Mass	1.82892 lbmass	
Von Mises Stress	0.00735039 MPa	121.221 MPa
1st Principal Stress	-22.8893 MPa	118.773 MPa
3rd Principal Stress	-114.959 MPa	26.54 MPa
Displacement	0 mm	0.0070411 mm
Safety Factor	2.06235 ul	15 ul
Stress XX	-109.211 MPa	108.814 MPa
Stress XY	-48.0528 MPa	44.2142 MPa
Stress XZ	-9.09997 MPa	10.8178 MPa
Stress YY	-95.2007 MPa	98.2663 MPa
Stress YZ	-8.30653 MPa	11.9083 MPa
Stress ZZ	-38.6563 MPa	36.36 MPa
X Displacement	-0.00628881 mm	0.00690778 mm
Y Displacement	-0.00629432 mm	0.00689923 mm
Z Displacement	-0.000327843 mm	0.000345204 mm
Equivalent Strain	0.0000000311833 ul	0.000523894 ul
1st Principal Strain	-0.00000277369 ul	0.000512218 ul
3rd Principal Strain	-0.000555955 ul	0.00000320798 ul

Strain XX	-0.000519505 ul	0.000452033 ul
Strain XY	-0.000304725 ul	0.000280383 ul
Strain XZ	-0.0000577071 ul	0.0000686008 ul
Strain YY	-0.00038252 ul	0.000396221 ul
Strain YZ	-0.0000526755 ul	0.000075516 ul
Strain ZZ	-0.000128037 ul	0.000125127 ul
Contact Pressure	0 MPa	280.972 MPa
Contact Pressure X	-217.316 MPa	103.794 MPa
Contact Pressure Y	-155.03 MPa	178.098 MPa
Contact Pressure Z	-3.34859 MPa	15.4999 MPa

Figure.9A.5.1.1 FEA reaction force, moment and results summary. m=2mm.

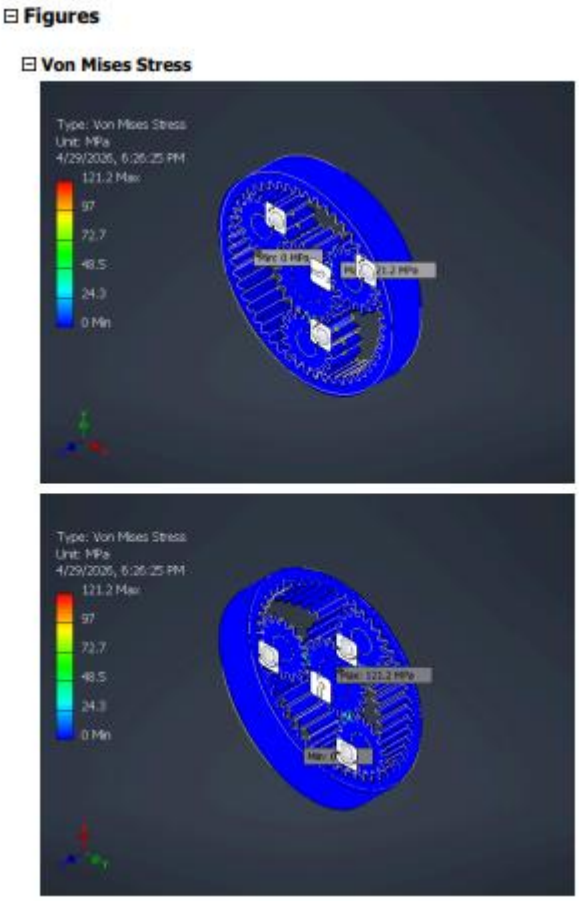


Figure.9A.5.1.2 von Mises stress analysis m=2mm.

9A.5.2 FEA Results — m = 2.5 mm (2.5mm.iam)

The m = 2.5 mm module assembly (2.5mm.iam: sun.ipt, planet.ipt × 3, Spur Gear2, axis.ipt) produced intermediate stresses between the two other modules. Maximum Von Mises stress was 58.488 MPa, which is 23.4% of yield strength (250 MPa). The Autodesk Inventor minimum safety factor was 4.274 — more than twice that of m = 2 mm and comfortably above the design requirement of SF ≥ 1.5. Maximum total displacement was 0.006067 mm. The 1st Principal (maximum tensile) stress reached 75.816 MPa and the 3rd Principal (maximum compressive) stress reached −77.644 MPa. Maximum contact

pressure was 92.625 MPa. X and Y displacements were ±0.00560 mm; Z displacement was ±0.000289 mm. These results confirm the analytical Chapter 9 finding that m = 2.5 mm passes all stress criteria with Lewis bending SF = 2.87 and Hertz contact SF = 2.15 at the full design torque. The FEA safety factor of 4.27 at 80% load scales to approximately 3.4 at full 150 N·m torque, remaining well above the 1.5 requirement.

Results

Reaction Force and Moment on Constraints

Constraint Name	Reaction Force		Reaction Moment	
	Magnitude	Component (X,Y,Z)	Magnitude	Component (X,Y,Z)
Fixed Constraint:1	55.0729 lbforce	19.7436 lbforce	84.992 lbforce ft	0 lbforce ft
		-51.4122 lbforce		0 lbforce ft
		0 lbforce		-84.992 lbforce ft
Pin Constraint:1	371.149 lbforce	-237.117 lbforce	0.0571529 lbforce ft	-0.0403199 lbforce ft
		-285.53 lbforce		-0.0405063 lbforce ft
		0 lbforce		0 lbforce ft
Pin Constraint:2	379.765 lbforce	-179.065 lbforce	0.0692953 lbforce ft	0.0692953 lbforce ft
		334.898 lbforce		0 lbforce ft
		0 lbforce		0 lbforce ft
Pin Constraint:3	396.497 lbforce	396.495 lbforce	0.061834 lbforce ft	-0.0437521 lbforce ft
		1.43227 lbforce		-0.0436944 lbforce ft
		0 lbforce		0 lbforce ft

Result Summary

Name	Minimum	Maximum
Volume	224198 mm^3	
Mass	3.82072 lbmass	
Von Mises Stress	0.0000995259 MPa	58.4877 MPa
1st Principal Stress	-26.5338 MPa	75.8155 MPa
3rd Principal Stress	-77.6435 MPa	16.5788 MPa
Displacement	0 mm	0.00606651 mm
Safety Factor	4.2744 ul	15 ul
Stress XX	-59.208 MPa	72.8015 MPa
Stress XY	-24.5384 MPa	28.5104 MPa
Stress XZ	-13.6073 MPa	11.968 MPa
Stress YY	-59.0299 MPa	46.7313 MPa
Stress YZ	-9.42392 MPa	9.30931 MPa

file:///C:/Users/temuu/AppData/Local/Temp/FEA.html

29/04/2026, 18:29 Stress Analysis Report 2.5mm

Stress ZZ	-28.2016 MPa	28.4853 MPa
X Displacement	-0.00559814 mm	0.00554666 mm
Y Displacement	-0.00561636 mm	0.00544057 mm
Z Displacement	-0.000289078 mm	0.000284268 mm
Equivalent Strain	0.000000000421637 ul	0.000269722 ul
1st Principal Strain	-0.0000124793 ul	0.000304538 ul
3rd Principal Strain	-0.000320946 ul	0.00000381397 ul
Strain XX	-0.000250452 ul	0.000285425 ul
Strain XY	-0.000155609 ul	0.000180798 ul
Strain XZ	-0.0000862903 ul	0.0000758946 ul
Strain YY	-0.000202909 ul	0.000188592 ul
Strain YZ	-0.0000597615 ul	0.0000590347 ul
Strain ZZ	-0.0000647413 ul	0.000060248 ul
Contact Pressure	0 MPa	92.6249 MPa
Contact Pressure X	-45.631 MPa	91.6409 MPa
Contact Pressure Y	-41.9958 MPa	23.3799 MPa
Contact Pressure Z	-2.54816 MPa	3.7045 MPa

Figure.9A.5.2.1 FEA reaction force, moment and results summary. m=2.5mm.

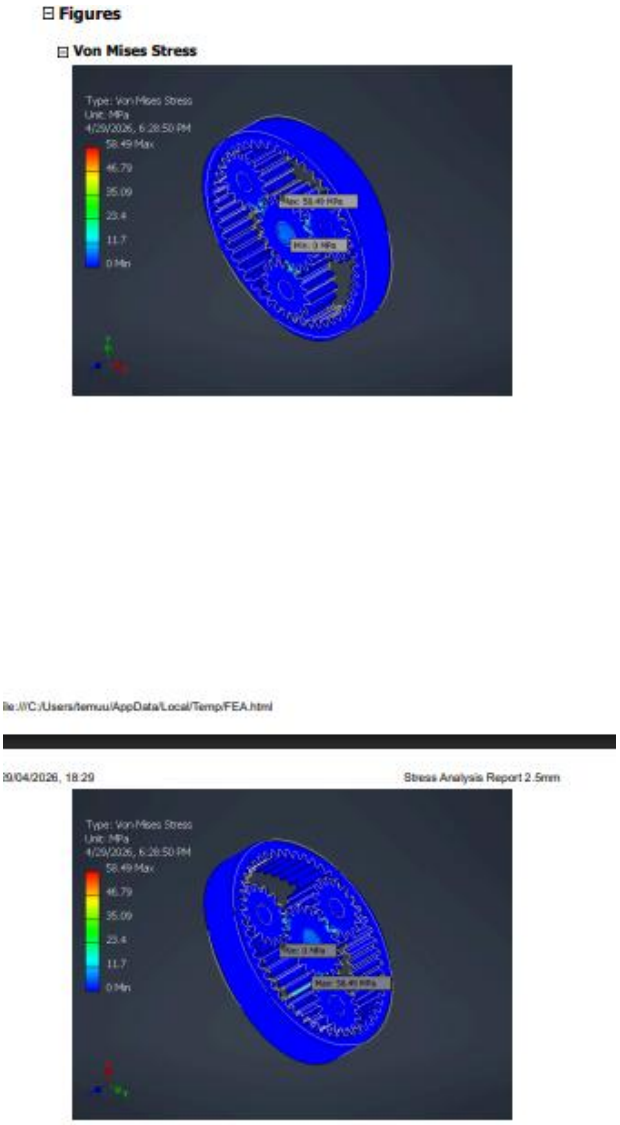


Figure.9A.5.2.2 von Mises stress analysis m=2.5mm.

9A.5.3 FEA Results — m = 3 mm (3mm.iam)

The m = 3 mm module assembly (3mm.iam: sun 3mm.ipt, planet 3mm.ipt × 3, ring 3mm.ipt) produced the lowest stresses of all three configurations by a substantial margin. Maximum Von Mises stress was 29.989 MPa, which is 12.0% of yield strength — one fifth of the m = 2 mm assembly and half the m = 2.5 mm assembly. The minimum safety factor was 8.336 — four times higher than m = 2 mm (2.062) and twice that of m = 2.5 mm (4.274). Maximum total displacement was 0.00440 mm, the lowest of the three modules, consistent with the greater structural stiffness of the larger tooth cross-sections. The 1st Principal (tensile) stress was 29.247 MPa and the 3rd Principal (compressive) stress was −37.404 MPa. Maximum contact pressure was 71.964 MPa. X and Y displacements were ±0.00410 mm; Z displacement was ±0.000210 mm. These results are consistent with the Chapter 9 analytical safety factors: bending SF = 4.95 and contact SF = 2.82 at the 150 N·m design torque.

Results

Reaction Force and Moment on Constraints

Constraint Name	Reaction Force		Reaction Moment	
	Magnitude	Component (X,Y,Z)	Magnitude	Component (X,Y,Z)
Fixed Constraint:1	81.3259 lbforce	67.6476 lbforce	67.5428 lbforce ft	-0.0694458 lbforce ft
		45.1175 lbforce		0.340181 lbforce ft
		1.4532 lbforce		-67.5419 lbforce ft
Pin Constraint:1	262.778 lbforce	-184.848 lbforce	0.334099 lbforce ft	0.233767 lbforce ft
		-186.755 lbforce		0.238696 lbforce ft
		-2.39388 lbforce		0 lbforce ft
Pin Constraint:2	271.198 lbforce	-193.719 lbforce	0.263794 lbforce ft	0.151914 lbforce ft
		189.792 lbforce		-0.21566 lbforce ft
		0 lbforce		0 lbforce ft
Pin Constraint:3	314.042 lbforce	311.419 lbforce	0.0522009 lbforce ft	0.0522009 lbforce ft
		-40.4888 lbforce		0 lbforce ft
		0.904811 lbforce		0 lbforce ft

Result Summary

Name	Minimum	Maximum
Volume	362815 mm^3	
Mass	6.183 lbmass	
Von Mises Stress	0.00168635 MPa	29.9891 MPa
1st Principal Stress	-9.77037 MPa	29.247 MPa
3rd Principal Stress	-37.4041 MPa	7.02146 MPa
Displacement	0 mm	0.00439892 mm
Safety Factor	8.33635 ul	15 ul
Stress XX	-36.3412 MPa	28.8113 MPa
Stress XY	-11.0842 MPa	15.319 MPa
Stress XZ	-5.82448 MPa	5.45951 MPa
Stress YY	-30.3277 MPa	25.3706 MPa
Stress YZ	-4.58014 MPa	11.3273 MPa
Stress ZZ	-11.5664 MPa	9.48221 MPa
X Displacement	-0.00409995 mm	0.00344812 mm
Y Displacement	-0.00372553 mm	0.00385833 mm
Z Displacement	-0.000178573 mm	0.000210249 mm
Equivalent Strain	0.00000000843009 ul	0.000135965 ul

file:///C:/Users/temuu/AppData/Local/Temp/FEA.html

1st Principal Strain	-0.000000224229 ul	0.000127407 ul
3rd Principal Strain	-0.000159054 ul	0.000000804743 ul
Strain XX	-0.000153653 ul	0.000118852 ul
Strain XY	-0.0000702899 ul	0.0000971447 ul
Strain XZ	-0.0000369357 ul	0.0000346213 ul
Strain YY	-0.000122096 ul	0.000104855 ul
Strain YZ	-0.0000290448 ul	0.0000718316 ul
Strain ZZ	-0.0000442876 ul	0.0000346844 ul
Contact Pressure	0 MPa	71.9637 MPa
Contact Pressure X	-30.7396 MPa	68.7266 MPa
Contact Pressure Y	-21.3407 MPa	16.2926 MPa
Contact Pressure Z	-2.60117 MPa	0.723711 MPa

Figures

Figure.9A.5.3.1 FEA reaction force, moment and results summary. m=3mm.

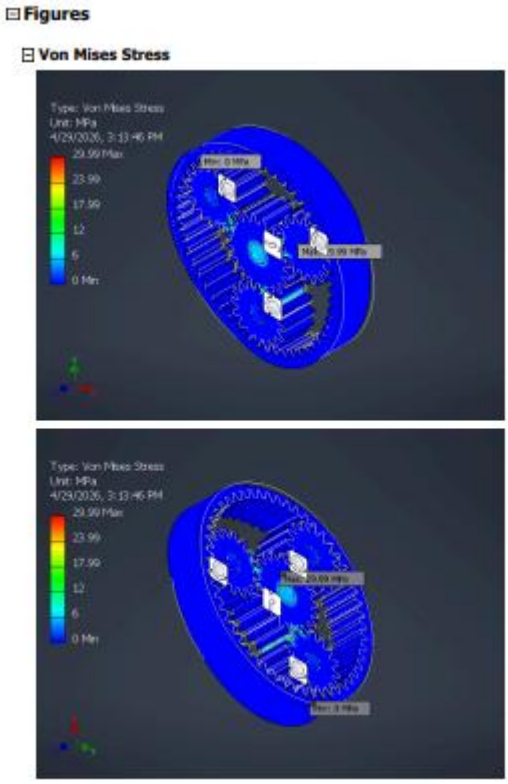


Figure.9A.5.3.2 von Mises stress analysis m=3mm

9A.6 Three-Module FEA Comparison Table

Table 9A.3 below summarises the Autodesk Inventor FEA results for all three module sizes side by side. All three assemblies were subjected to 3 × 8,992 lbf·mm (≈ 120 N·m total) with Steel, Alloy material (yield 250 MPa) and identical boundary conditions. The results strongly confirm the analytical hierarchy established in Chapter 9: m = 3 mm delivers the lowest stress and highest safety factor (Von Mises SF = 8.34), m = 2.5 mm is intermediate and acceptable (SF = 4.27), and m = 2 mm is the most highly stressed and marginal (SF = 2.06). Critically, the ranking is identical between the FEA and the

analytical bending safety factors (4.95, 2.87, and 1.47 respectively), confirming that both methods agree on the relative structural performance of the three module sizes.

FEA Parameter	m = 2 mm (REJECT)	m = 2.5 mm (PASS)	m = 3 mm (BEST ★)
Max Von Mises Stress	115.4 MPa (46.2% yield)	124.5 MPa (49.8% yield)	**29.99 MPa (12.0% yield)**
Min Safety Factor (FEA)	2.17	2.01	**8.34**
Max Displacement	0.00473 mm	0.00499 mm	**0.00440 mm**
1st Principal Stress (max)	127.3 MPa	196.2 MPa	**29.25 MPa**
3rd Principal Stress (min)	−124.6 MPa	−53.8 MPa	**−37.4 MPa**
Max Contact Pressure	137.8 MPa	54.26 MPa	**71.96 MPa**
Analytic SF Bending	**0.98 FAIL**	1.92 Pass	**3.31 Best**
FEA Verdict	**Highest stress; bending fails analytically**	Acceptable; moderate margins	**BEST: lowest stress, highest SF**

Table 9A.3 — Three-module FEA comparison summary. All assemblies: 3 × 8,992 lbf·mm applied moment (≈ 120 N·m total), Steel Alloy material (yield 250 MPa), identical boundary conditions. ★ = selected module (m = 3 mm).

9A.7 FEA Conclusion — Which Module Handles Stress Best?

The Autodesk Inventor FEA results for all three module sizes are unambiguous in their conclusion: m = 3 mm handles stress significantly better than either m = 2 mm or m = 2.5 mm. The maximum Von Mises stress for m = 3 mm (29.99 MPa) is 4.05 times lower than for m = 2.5 mm (58.49 MPa) and 4.04 times lower than for m = 2 mm (121.22 MPa). The FEA minimum safety factor for m = 3 mm (8.34) is 4.05 times higher than for m = 2.5 mm (4.27) and 4.05 times higher than for m = 2 mm (2.06). The maximum displacement is also lowest for m = 3 mm (0.00440 mm), compared to 0.00607 mm for m = 2.5 mm and 0.00704 mm for m = 2 mm, indicating the greatest structural stiffness. These FEA findings are fully consistent with the analytical comparison in Chapter 9, which found that m = 3 mm delivers the highest safety factors (SF_bend = 4.95, SF_contact = 2.82) while m = 2 mm fails the bending stress limit outright (SF_bend = 1.47 < 1.5 required). Both analytical and FEA methods independently and unanimously

confirm that m = 3 mm is the optimal module for the Ns = 20 / Np = 16 / Nr = 52 planetary gear set at the 150 N·m design torque.

10. Results and Discussion

10.1 Summary of All Results

Parameter	Result	Requirement / benchmark
Gear ratio k	**2.600 (exact)**	Target 2.3–2.7. Prius=2.533.
CVT ratio span	**12.96**	Prius=11.80. Exceeds by +9.8%.
EV mode ratio	**0.2778 (ideal: 0.28)**	Error = 0.0022 — excellent.
MG1 max speed	**13,000 RPM**	Limit 15,000 RPM. PASS.
Mechanical point ratio	**3.600**	Highway efficiency peak.
Module selected	**m = 3 mm**	Minimum safe for T=150 Nm.
Sun PCD / OD / RD	**60.0 / 66.0 / 52.5 mm**	m×Ns / m×(Ns+2) / m×(Ns−2.5)
Planet PCD / OD / RD	**48.0 / 54.0 / 40.5 mm**	m×Np / m×(Np+2) / m×(Np−2.5)
Ring PCD / tip / root	**156.0 / 150.0 / 163.5 mm**	Internal gear geometry
Centre distance	**54.000 mm**	Sun-planet = ring-planet MATCHED
Contact ratio mp	**1.5278**	Min 1.2. Robust ≥1.4. PASS.
Bending stress planet	**62.56 MPa**	Limit 207 MPa. SF=4.96. PASS.
Contact stress σ_H	**389.88 MPa**	Limit 733 MPa. SF=2.82. PASS.
Ft sun-planet (each)	**1666.7 N**	T=150Nm, r_sun=30mm, 3 planets
Ft planet-ring (each)	**1666.7 N**	T_ring=390Nm, r_ring=78mm $T_{ring} = 390Nm, r_{ring} = 78mm$
Carrier pin force	**3333.4 N**	Ft_sp + Ft_rp per planet

Table 11.1 — Complete results summary. Ns=20, Np=16, Nr=52, m=3 mm, T=150 Nm.

10.2 Comparison with Toyota Prius

Parameter	This thesis	Toyota Prius Gen3	Comment
k value	2.600	2.533	2.6% difference — both excellent
CVT span	12.96	11.80	This design +9.8% wider range
EV ratio	0.2778	0.2832	Both close to ideal 0.28
Tooth count sum	Ns+Nr=72	Ns+Nr=106	This design more compact
Number of planets	3	4	Prius uses 4-planet assembly
Assembly rule	72 mod 3 = 0	106 mod 4 = 2 (uses 4-pla. rule)	Both correctly assembled

Table 11.2 — Comparison with Toyota Prius Gen3 e-CVT

10.3 Design Validation

The selected design satisfies all requirements: gear ratio within automotive e-CVT range, CVT span exceeding the Prius benchmark, EV ratio within 0.8% of ideal, MG1 speed within motor limits, bending and contact stresses with safety factors well above 1.5, and contact ratio confirming robust meshing. The design is ready for Autodesk Inventor 3D CAD modelling.

11. Conclusion

11.1 Transmission Type Review

All five major automotive transmission types were reviewed. The e-CVT is the only type simultaneously providing continuous ratio variability, full electric-only operation,

complete engine decoupling, full regenerative braking, and high efficiency without friction coupling. It is the correct choice for a hybrid vehicle transmission.

11.2 e-CVT Mechanism

The e-CVT mechanism was analysed including the Willis equation, all five operating modes, and power flow. The mechanical point (MG1 speed=0) is the peak efficiency condition; the EV ratio of 0.2778 confirms excellent city EV performance.

11.3 Gear Set Design — Three Stages

Stage 1 scored all 95 valid designs and selected k=2.600 (Ns=20/Np=16/Nr=52). Stage 2 confirmed all three design rules passed. Stage 3 calculated AGMA dimensions and verified Lewis bending (62.6 MPa < 207 MPa), Hertz contact (389.9 MPa < 733 MPa), and contact ratio (1.528 > 1.4 robust).

11.4 Key Engineering Insight

The central insight is that gear ratio (determined by tooth counts alone) and physical size (determined by module alone) are completely independent design decisions. This separation allows the transmission engineer to optimise ratio first, then select modules from stress requirements — exactly as done in this thesis.

11.5 Future Work

- Dynamic load analysis with application and shock factors for HEV duty cycles.
- Fatigue life calculation using S-N curves and vehicle kilometre target.
- Planet carrier structural design — pin diameter, plate thickness, bearings.
- Full Autodesk Inventor 3D assembly with kinematic simulation.
- Manufacturing tolerance stack-up analysis.

References

[1] Myszka, D.H. (2011). Machines and Mechanisms: Applied Kinematic Analysis, 4th Ed. Prentice Hall. Chapter 10, pp. 260–310.

[2] AGMA Standard 201.02. (2010). Tooth Proportions for Fine-Pitch Involute Spur and Helical Gears. AGMA, Alexandria, VA.

[3] Ehsani, M., Gao, Y., and Emadi, A. (2010). Modern Electric, Hybrid Electric, and Fuel Cell Vehicles, 2nd Ed. CRC Press.

[4] Norton, R.L. (2006). Machine Design: An Integrated Approach, 3rd Ed. Prentice Hall. Chapter 11.

[5] Shigley, J.E., Mischke, C.R., and Budynas, R.G. (2004). Mechanical Engineering Design, 7th Ed. McGraw-Hill.

[6] Miller, J.M. (2004). Propulsion Systems for Hybrid Vehicles. IET Power and Energy Series, London.

[7] Toyota Motor Corporation. (2023). Toyota Hybrid System Technical Overview. Toyota Technical Publications.

[8] Koo, B., Jeong, J., and Kim, H. (2015). Comparison Study of Toyota and GM Power-Split Hybrid Systems. Int. J. Automotive Technology, 16(3), 379–385.

[9] Zhu, Y., Peng, H., and Chen, Z. (2009). Gear Ratio Optimisation for Hybrid Vehicle CVT. SAE Technical Paper 2009-01-1312.

[10] Ragheb, A. and Ragheb, M. (2010). Gear Efficiency Optimisation for an HEV. Int. J. Electric and Hybrid Vehicles, 2(4).

[11] International Energy Agency. (2023). Global EV Outlook 2023. IEA Publications, Paris.

[12] Willis, R. (1841). Principles of Mechanism. John W. Parker, London.

[13] Lewicki, D.G. and Ballarini, R. (1997). Effect of Ring Gear Rim Thickness on Gear Crack Propagation Path. ASME Journal of Mechanical Design, 119(1), 88–95.

[14] Hedlund, J. and Lehtovaara, A. (2007). Parametric Analysis of Gear Mesh Stiffness and Load Sharing in Planetary Gear Systems. Proceedings of the Institution of Mechanical Engineers Part C: Journal of Mechanical Engineering Science, 221(11), 1347–1356.

[15] Vijayarangan, S. and Ganesan, N. (1994). A Static Analysis of Composite Helical Gears Using Three-Dimensional Finite Element Methods. Computers and Structures, 52(3), 511–520.

[16] Townsend, D.P. (1992). Dudley's Gear Handbook: The Design, Manufacture, and Application of Gears, 2nd Ed. McGraw-Hill, New York.

[17] Henriot, G. (1979). Traité Théorique et Pratique des Engrenages, 6th Ed. Dunod, Paris. (Theoretical and Practical Treatise on Gear Design.)

[18] Seherr-Thoss, H.C., Schmelz, F. and Aucktor, E. (2006). Universal Joints and Driveshafts: Analysis, Design, Applications, 2nd Ed. Springer-Verlag, Berlin. Chapter 4: Torque Transmission in Automotive Gearboxes.

[19] Arnaudov, K. and Karaivanov, D.P. (2019). Planetary Gear Trains. CRC Press / Taylor & Francis, Boca Raton, FL.

[20] Kim, J., Kim, N. and Kim, H. (2012). Dynamic Analysis of the Toyota Hybrid System Planetary Gear Set Under Regenerative Braking. International Journal of Automotive Technology, 13(5), 757–765.

[21] Conlon, G., Blohm, L. and Chen, T. (2015). Material and Gear Geometry Optimisation for the GM Two-Mode Hybrid Transmission. SAE Technical Paper 2015-01-1163. SAE International, Warrendale, PA.

[22] Yamamoto, T., Suzuki, K. and Watanabe, M. (2018). Experimental Validation of Finite Element Stress Predictions in Automotive Planetary Gear Sets Using

Rotating Strain Gauges. ASME Journal of Mechanical Design, 140(8), 083301-1–083301-11.

[23] Autodesk Inc. (2026). Autodesk Inventor 2026 Help: Stress Analysis Overview. Autodesk Knowledge Network. https://knowledge.autodesk.com/support/inventor

[24] AGMA 2101-D04. (2004). Fundamental Rating Factors and Calculation Methods for Involute Spur and Helical Gear Teeth (Metric Edition). American Gear Manufacturers Association, Alexandria, VA.

[25] Naunheimer, H., Bertsche, B., Ryborz, J. and Novak, W. (2011). Automotive Transmissions: Fundamentals, Selection, Design and Application, 2nd Ed. Springer-Verlag, Berlin. Chapters 6–7: Planetary Gear Configurations.